Global distribution of modern shallow marine shorelines. Implications for exploration and reservoir analogue studies

Björn Nyberg[1,2*], John A. Howell[3]

Uni Research CIPR, P.O. Box 7810, 5020 Bergen Norway.[1]

Department of Earth Sciences, University of Bergen, P.O. Box 7803, 5020 Bergen, Norway.[2]

Department of Geology and Petroleum Geology, University of Aberdeen, Meston Building, Old Aberdeen, AB24 3UE UK[3]

*Corresponding author: bjorn.burr.nyberg@gmail.com

Abstract

Deposits of marginal marine depositional systems make up significant hydrocarbon reservoirs in the rock record. These systems are deposited by a complex interaction between competing depositional processes which can result in heterogeneous and compartmentalised reservoirs. Shallow marine systems are described using a ternary classification describing the relative importance of wave, tide and fluvial processes at the coastline. With the advent of freely available remote sensing data, modern systems are being increasingly used as analogues for the ancient, however to date, there has been no systematic quantification of global modern paralic systems. The aim of the present study has been to map and classify all the world's shorelines by ternary process and to consider the distribution and controls on different shoreline types.

The semi-automated classification of marginal marine clastic shorelines has been achieved by combining data from a series of proxies for the ternary processes. Combined with coastline morphology, an algorithm predicts shoreline classification with an 85% success rate when compared to manual interpretation. Using this algorithm, the global shoreline has been

subdivided into 246,777, 5km segments and the distribution and proportions of these analysed.

The first order classification subdivides 28% of the world's coastlines as depositional. Within the depositional coastlines 62% are Wave-dominated, 35% Tide-dominated and 3% Fluvial-dominated. Analysis of shoreline type distribution suggests a complex network of inter-related controlling factors. Of these, climate and tectonic setting are reasonably well constrained in the ancient and can be used to predict the probability of a specific shoreline type. In addition to shedding insight into the controls on the distribution of different shoreline types, the results of this study can also be used to identify suitable modern analogues for ancient systems, which in turn can be used to extract data for better reservoir characterisation.

KEYWORDS: modern analogues; modern depositional environments; marginal marine; ternary process; petroleum plays

1. Introduction

Within sedimentology, paralic and shallow marine depositional systems are traditionally described using a ternary classification based upon the relative importance of fluvial, tidal and wave processes on sculpting the shoreline geomorphology (Galloway, 1975). The different processes will drastically impact the morphology and distribution of sandbodies within a depositional environment and introduce heterogeneity into shallow marine reservoirs (Hampson and Storms, 2003; Ainsworth et al., 2008; Howell et al., 2008; Ainsworth et al., 2011). The advent of freely available, moderate to high quality, remote sensing data has seen a significant increase in the use of modern systems as analogues for the rock record and for hydrocarbon reservoirs in particular. Understanding the distribution of modern shoreline systems and the controls on these distributions at a global scale is therefore highly desirable.

Paralic and shallow marine systems may be classified in a number of different ways. In addition to the ternary plot of Galloway (1975) it is also useful to consider whether the shoreline is in net deposition or net erosion over several distinct timescales. Boyd et al. (1992) subdivided shorelines on whether they were progradational or transgressive noting that there are significant differences in sediment body geometry and distribution between the two. Progradational shorelines occur where sediment supply exceeds accommodation and the shoreline moves basinward through time. They are typically deltas or strandplains. Transgressive shorelines, in which accommodation is greater than sediment supply and the shoreline moves landward through time are dominated by barrier islands and estuaries. In addition to the systems described by Boyd et al. (1992), there are also “rocky shorelines” or “high relief transgressive” shorelines (sensu Howell, 2005) which are parts of the coast that are in long term, net erosion over timescales of millions of years. These were not included in the classifications of Galloway (1975) or Boyd et al. (1992) because they do not become a part of the geological record except as unconformity surfaces, their recognition is however important in the modern since they account for a significant proportion of modern coastlines.

Prior to the work of Galloway (1975), Wright and Coleman (1973) classified systems based upon the relative importance of fluvial vs “basinal” processes, this work was superseded by the Galloway (1975) classification. Orton and Reading (1993) extended the ternary plot into a 3rd dimension with grainsize as the additional parameter. Most significantly Ainsworth et al. (2011) further subdivided the ternary diagram and added a systematic method for the description and classification of shorelines which is described below.

Here we present a global classification of shoreline type based upon previously available data on the distribution of wave and tidal processes and, newly generated data on the relative importance of fluvial processes at and away from specific fluvial input points. These

parameters have been quantitatively combined to generate a global classification of shoreline type, based upon the first two levels (dominated and influenced) of Ainsworth et al.'s (2011) modification of Galloway's (1975) classification scheme. The results of this global classification can be used to define the importance of parameters such as shelf width, climate, structure, latitude and basinal energy in controlling shoreline type. The resultant maps can also be filtered by parameters such as climate and basin type in order to locate suitable modern analogues for ancient systems.

2. Previous work on global classification of shorelines

The coastal environment is a dynamic zone which lies between the sub-aerial and sub-aqueous realms. From social, economic, climatic, ecological, biochemical and sea-level perspectives; it has been the subject of significant research interest (Costanza et al., 1998; Crossland et al., 2003; Talaue-McManus et al., 2003; Jorgenson and Brown, 2005; Buddemeier et al., 2008; Vafeidis et al., 2008; Bird et al., 2013). The nomenclature used to subdivide and classify shorelines typically reflects the needs of the specific field or study. Previous efforts to produce global shoreline typologies include the LOICZ project for biochemical coastal zonation (Crossland et al., 2003; Buddemeier et al., 2008); vulnerability to sea-level rise (Vafeidis et al., 2008) and littoral marine habitat (Bird et al., 2013) databases. To date there has been very few attempts at global classification of shoreline type in a framework that is appropriate to sedimentology and geomorphological.

The first global classification of shoreline by geomorphology and tectonics was by Inman and Nordstrom (1971). This study classified shorelines as mountainous, narrow-shelf, wide-shelf, deltaic, reef or glaciated coasts, within the newly emergent field of plate tectonics, placing them in collisional, trailing edge and marginal sea settings. Second order classifications subdivide these geomorphological categories into wave erosion, wave

deposition, river deposition, wind deposition, glaciated and biogenous at scales of approximately ~100km. Dürr et al. (2011) has expanded and digitized the geomorphological classification of coastlines to categorize regionally, locations of small deltas, large rivers, estuaries, lagoons, tidal systems, arheic settings and fjords. Focusing on the application of global fluvial discharge to estuaries, the study is defined at 0.5 degrees (approximately 50km) using the boundaries of watershed basins by Vörösmarty et al., (2000a, b) as its shoreline delineation. In addition, the shoreline classification does not aim to characterize any regional scale variability in its analysis of shoreline geomorphology. Hence while shorelines are segmented at scales of 50km, its dominant classification are typically at scales similar to the delineation by Inman and Nordstrom (1971). For our purpose, these datasets do not provide the level of detail or appropriate nomenclature to efficiently identify suitable modern analogues of the marginal marine.

Regionally, Harris et al. (2002) demonstrated that a distinct statistical variation between wave height, tidal range and fluvial discharge can differentiate recognized classifications of shoreline geomorphology of the Australian coastline. Work by Short (2006) is the result of an impressive 17 year analysis of Australian shorelines (1987-2004) to classify 15 shoreline geomorphologies and their association to four main processes of Wave-dominated, Tide-dominated, Tide-modified and beaches on rocky/coral flats based on tidal range, breaking wave height and manual interpretation of regional maps and aerial photography. Also in Australia, Nanson et al. (2013) made a detailed, manual classification of the marginal marine depositional elements in the Mitchell delta, Gulf of Carpentaria, using the hierarchical and ternary process classification scheme of Ainsworth et al. (2011). Vakarelov and Ainsworth (2011) used the same classification scheme to classify 416 marginal marine systems in Asia by ternary process. To apply a similar manual interpretation at a global scale is impractical. To our knowledge, no previous global classification of shorelines by ternary process currently exists.

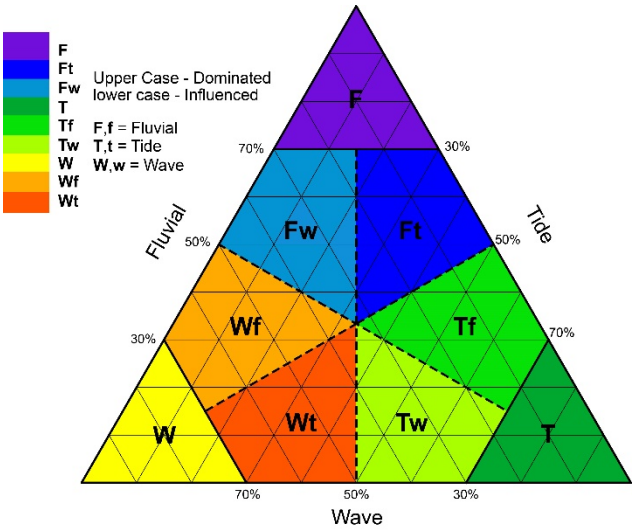

Figure 1. A two tier ternary plot modified after Ainsworth et al. (2011) to classify shoreline type as dominated and influenced based on the relative percentage of wave, fluvial and tidal processes acting on a stretch of coastline. These include; F - Fluvial-dominated, Ft - Fluvial-dominated Tide-influenced, Fw - Fluvial-dominated Wave-influenced, T - Tide-dominated, Tf - Tide-dominated Fluvial-influenced, Tw - Tide-dominated Wave-influenced, W - Wave-dominated, Wf - Wave-dominated Fluvial-influenced and Wt - Wave-dominated Tide-influenced.

The challenge that remains is to apply the ternary process classification (Galloway, 1975; Ainsworth et al., 2011) to the coastlines of the entire world. The goal here is to devise a global ternary plot classification using an automated approach that limits subjective bias and allows for a quantitative study of controlling parameters.

3. Ternary classification of shallow marine systems

The ternary diagram of Galloway (1975) relates the relative influence of fluvial, tide and wave processes on the classification of deltaic environments. Subsequent ternary plot classifications have expanded that concept to describe the range of marginal marine depositional environments (Boyd et al., 1992; Ainsworth et al., 2011). Recent work by Ainsworth et al. (2011) and Vakarelov and Ainsworth (2013) have incorporated a semi-quantitative method to categorize ancient and modern marginal marine systems by the proportion of elements associated with each process. In this schema they also added two additional degrees of granularity describing dominant, influencing and affecting for the main, second order and third order processes on a given shoreline. This schema then states a depositional environment is classified first by the dominant ternary process (W, T or F; e.g., Fluvial-dominated; **F**), then by the secondary process (e.g., Fluvial-dominated, Tide-influenced; **F**t) and finally by the tertiary process (e.g., Fluvial-dominated, Tide-influenced and Wave-affected; **F**t*w*). This schema gives 15 possible classes.

3.1. Predictive ternary process classification

For the purpose of the current worldwide study, we have used a predictive two-tier ternary process classification (dominated and influenced; Figure 1) that is modified from Galloway (1975) and Ainsworth et. al (2011). The classification is calculated from the relative strength of the different processes based upon global datasets for each. This predictive two-tier ternary process classification quantifies the tide, wave and fluvial power acting on a stretch of shoreline to predict the dominated and influenced ternary processes on coastline geomorphology. This modified approach relies on the relative power of the various ternary process rather than the preserved volumetric or aerial proportions of sandbody deposits by ternary process (e.g., Ainsworth et al. 2011). The benefit of the current approach is that it is

automated, auditable, predictive and once established, very fast.

While there is scope to extend this modified classification (Figure 1) to a three-tier scheme (i.e. Ainsworth et al. 2011), our initial work suggests that it adds additional ambiguity in defining the thresholds that separates a dominated versus influenced versus affected ternary process system. Those thresholds are difficult to capture given the limitations in data resolution in this global study. The two-tier ternary process classification we have used describes 9 different shoreline types (**F**, **Ft**, **Fw**, **T**, **Tf**, **Tw**, **W**, **Wf** and **Wt**; Figure 1). The heterogeneity and compartmentalization associated with each shoreline type is important to understanding their potential subsurface reservoir behavior (Hampson and Storms, 2003; Howell et al., 2008).

3.2. Ternary process classifications

Fluvial-dominated (**F**) shorelines, Figure 2a, are generally characterized by progradational deltas dominated by a fluvial process with only very minor wave or tidal reworking. They range in size from small to very large systems dependent on the size of the river discharge. These reservoir systems are composed mainly of mouth-bar sandstones cut by distributary channel deposits. The presence of dipping clinoforms in the mouthbars will impact reservoir performance (Howell et al., 2008). A typical modern example is the Mississippi delta or the Wax Lake delta (Wellner et al., 2005) in the Gulf of Mexico. The Ferron Sandstone in Ivie Creek, Utah is an excellent outcrop example (Enge and Howell, 2010; Deveugle et al., 2014).

Fluvial-dominated *Tide-influenced* (**Ft**) shorelines (Figure 2b) are characterized by a deltaic environment that illustrates a strong tidal influence which manifests in the geometry of the distributary channels which are strongly funnel shaped. There are also a series of tidal channels, flats and floodplains on the delta plain. Tidal bars are typically elongated

perpendicular to shoreline sandbodies and mouthbars may include a degree of tidal reworking and modification. Modern **Ft** examples include the active fluvial portions of the Mekong delta, Vietnam, the Irrawaddy delta Myanmar and the Ganges-Brahmaputra delta, India/Bangladesh (Goodbred and Saito, 2012). Reservoir modeling considerations are similar to those of Fluvial-dominated deltas although channels and mouth-bars may be more heterolithic with more mud draped bedforms.

Fluvial-dominated *Wave-influenced* (**Fw**) shorelines, Figure 2c, are characterized by a deltaic protrusion on the coastline that is heavily modified by wave action. Sediment introduced by the fluvial system is reworked along strike by wave activity. There are a limited number of distributary channels and the mouthbar(s) are heavily modified by wave action. Away from the fluvial entry point the shoreline is dominated by linear sand dominated shorefaces. Beach ridges are common. In systems with a strong component of longshore drift there may be a difference between the shoreline systems on the updrift and down drift sides of the input point (Bhattacharya and Giosan 2003). The reservoir quality associated with **Fw** systems produces excellent quality reservoirs similar to Wave-dominated shorelines although locally there may be increased intra-shoreface shales near the river mouth (Eide et al. 2014). Many modern **Fw** systems are protruding fluvial mouth shorelines of a larger Wave-dominated delta including the Paraiba do Sul delta in Brazil and the Usumacinta - Grijalva delta in Mexico.

Tide-dominated (**T**) shorelines, Figure 2d, are characterized by funneled branching tidal channels, tidal bars, tidal mudflats and salt marshes unassociated with any fluvial influence. In the sub-tidal region, migrating sub-tidal dunes lie within sub-aqueous channels bordered by large sand flats. Landward, the inter-tidal zone is typified by an increasingly mud-dominated and sandy heteroliths. Modern examples include the western portions of the Ganges delta in Bangladesh and India. Due to the heterolithic nature of Tide-dominated deposits, these

systems make challenging reservoirs though sub-tidal portions may make good reservoirs that are otherwise flanked by a heterogenous inter-tidal zone (McIlroy et al., 2005; Martinius et al 2014).

Tide-dominated *Fluvial-influenced* (**Tf**) shorelines, Figure 2e, are similar to Tide-dominated shorelines exhibiting branching and funneled channels, sub-aqueous and sub-aerial tidal bars, tidal flats and floodplains and salt marshes. The main difference is presence of a fluvial component to the system which introduces sediment to the near-shore environment which is then reworked into tidal bars, channels and flats. The distinction between **Tf** and **Ft** is that in the **Tf** the fluvial input is not significant enough to prograde a prominent mouthbar. The shoreline associated with the foreland basin of southern Papa New Guinea is a good modern example of a Tide-dominated system that is locally influenced by fluvial input. Reservoirs face similar challenges to those in Tide-dominated systems whereby the best quality reservoirs are potentially of the sub-tidal sand bedforms bounded laterally by the inter-tidal heterolithic zone. Fluvial sediment input may locally improve the reservoir quality of those heterolithic zones.

Tide-dominated *Wave-influenced* (**Tw**) shorelines, Figure 2f, are characterized by funneled channels associated with tidal bars, flats, floodplains and salt marshes that are wave-modified to include beach ridges and wave-generated shoreface deposits. In the sub-tidal region, tidal dunes and tidal channels are reworked by wave-generated storm processes. In the inter-tidal zone, tidal flats, floodplains and channels will be modified by wave action to create isolated fore-shore, beach and chenier ridge deposits that are often parallel to an open-body of water. Good quality reservoirs may be associated with these wave-modified shoreface sediments although heterolithc tidal deposits may impede reservoir production. Modern shoreline examples may include portions from the southern Gulf of Carpentaria in Australia or Western regions of Madagascar.

Wave-dominated (**W**) shorelines, Figure 2g, are characterized by linear shorefaces with land attached strandplains often with well-developed beach ridges. Sediment input is from longshore drift and erosion from a nearby erosional shoreline or fluvial output. As reservoirs these systems form excellent laterally extensive (strike) sandbodies that may form thick

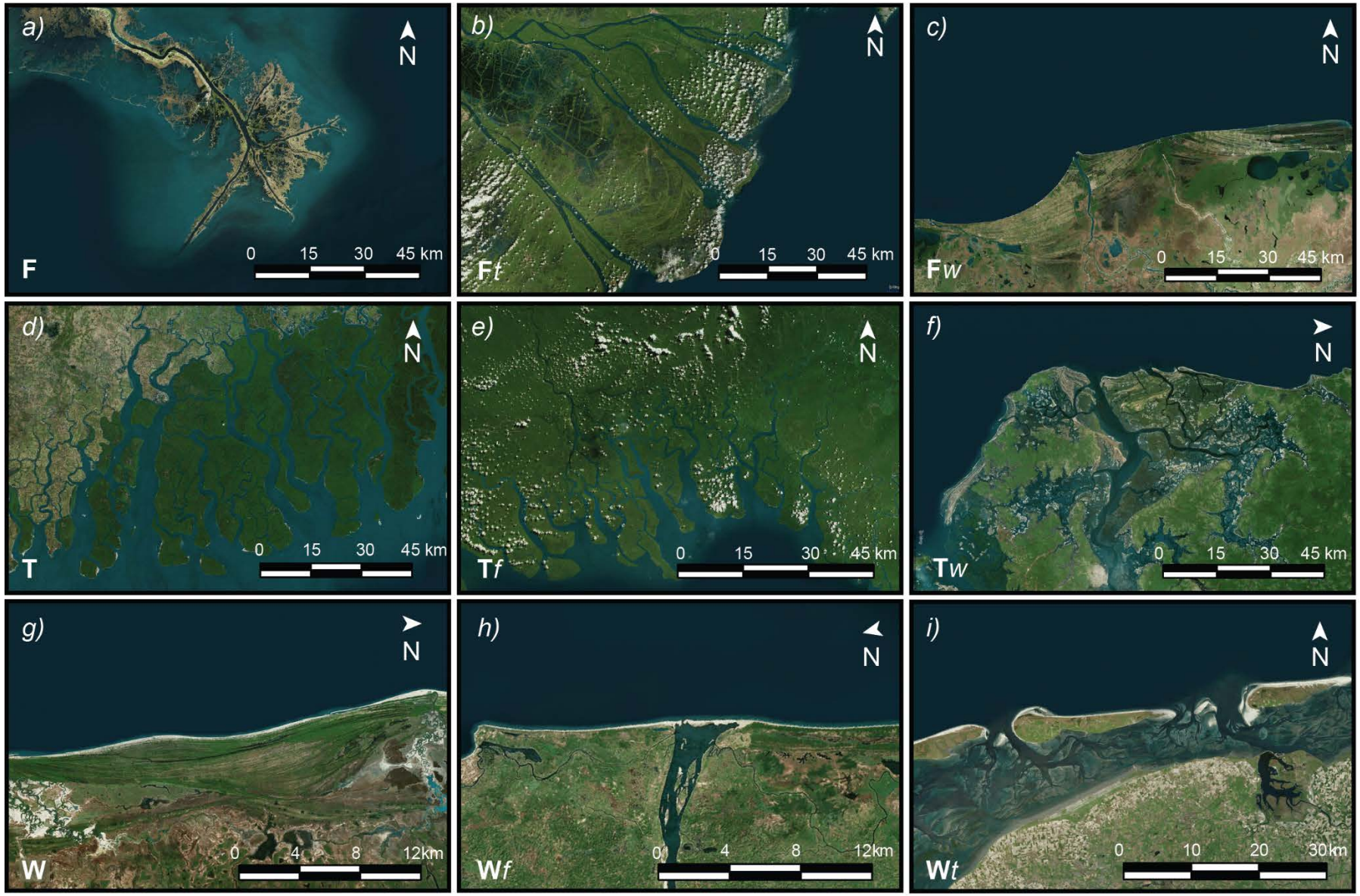
a)
N
0 15 30 45 km
F
b)
N
0 15 30 45 km
Ft
c)
N
0 15 30 45 km
Fw
d)
N
0 15 30 45 km
T
e)
N
0 15 30 45 km
Tf
f)
N
0 15 30 45 km
Tw
g)
N
0 4 8 12km
W
h)
N
0 4 8 12km
Wf
i)
N
0 10 20 30km
Wt

Figure 2. Examples of modern shorelines within the modified classification of Ainsworth et al. (2011) as used in this study. **a) – c)** display systems dominated by a fluvial component which are characterized by a protruding delta lobe. **a)** shows a Fluvial-dominated system (**F**) of the Mississippi delta in the Gulf of Mexico, USA. **b)** an example of Fluvial-dominated, Tide-influenced tidal delta on the Mekong delta, Vietnam. **c)** the protruding fluvial mouth portion of the Usumacinta - Grijalva delta in southern Mexico is a typical example of a Fluvial-dominated Wave-influenced (**Fw**) system. **d) – f)** are examples dominated by a tidal component characterized by a shoreline with an overall funnel shaped character. **d)** example of a Tide-dominated (**T**) shoreline from a fluvially inactive portion of the Ganges–Brahmaputra delta in eastern India/southern Bangladesh. **e)** an example of a Tide-dominated Fluvial-influenced system (**Tf**) is shown in eastern Papua New Guinea by numerous tidal channels fed by an active fluvial component. **f)** shows an example of a Tide-dominated Wave-influenced (**Tw**) system in Senegal, Western Africa which is characterized by a funnel shape with prominent beach ridge developments. **g) – i)** show modern systems dominated by wave activity characterized by a linear shoreface profile. **g)** shows a series of linear beach ridge complexes of a Wave-dominated (**W**) system of the northeastern Gulf of Carpentaria, Australia. **h)** a Wave-dominated Fluvial-influenced (**Wf**) shoreline from eastern Madagascar characterized by a linear shoreface profile with a fluvial input source. **i)** an example of a Wave-dominated Tide-influenced (**Wt**) system where a straight shoreface profile of a Wave-dominated barrier complex is in-cut by tidal channels. Imagery from Bing©.

successive sequences partitioned by flooding surfaces. In transgressive settings, Wave-dominated shorelines are barrier islands with similar shoreface profile on the seaward side and lagoons on the landward side. Modern examples may include the Nayarit, Mexico, Southern Brazilian coastline and much of the Gulf of Mexico coastline west of Florida.

Wave-dominated *Fluvial-influenced* (**Wf**) shorelines, Figure 2h, are similar to Wave-dominated shorelines with straight and parallel shoreface deposits with beach ridges. The minor fluvial influence does not generate a protruding delta and is often heavily modified by

the wave action. Modern day examples include many systems off the western coast of South America and eastern Madagascar. The subsurface behavior of these depositional environments is similar to the wave dominated systems, with fluvial input points producing minor heterogeneity.

Wave-dominated *Tide-influenced* (**Wt**) shorelines, Figure 2i, are characterized by shoreface systems with a greatly expanded foreshore and beach section, which is exposed at low tide (Vakarelov et al., 2012). The shoreface is also cut by sub-tidal channels. In embayed areas there may be minor tidal flats with tidal channels. Modern examples include many shorefaces of northern Australia and shorelines of West Africa. Many **Wt** reservoirs make excellent reservoirs that are very extensive in a strike direction, although they have greater heterogeneity than their wave dominated counterparts.

4. Methodology

The geometry of paralic and shallow marine sediment bodies is strongly controlled by the dynamic relationship of fluvial, tide and wave processes at the shoreline. The goal of this paper is to produce an automated global classification of modern shoreline type based upon available datasets which describe the distribution of these parameters.

When working at a global scale it is necessary to use numerous data sources, many of which will be proxies for the parameter that is ultimately required. Previous studies have used wave height and/or tidal range to predict geomorphology and/or ternary process at a shoreline (Davis Jr and Hayes, 1984; Harris et al., 2002; Short, 2006; Dürr et al., 2011). The current study combines improved data resolution with a mapped shoreline geometry to produce a much finer resolution and level of detail than has not been achieved by previous global studies (e.g. Dürr et al., 2011). This is achieved by segmenting the shoreline every 5 km's (Wessel and Smith, 1996) for subaerial polygonised landmasses greater than 250km^2 and mapping the

relative global ternary power influencing every stretch of shoreline (Figure 3). It is also important to note that the mapping reflects shorelines processes at the decadal timescale excluding episodic and seasonal variations, while also focusing on the process dominance at the shoreline now rather than mapping the long term evolution of a system. Greenland and Antarctica have been excluded from our analyses because of a lack of digital elevation models (DEM) which are required to calculate fluvial impact.

4.1. Sources of data

Data applied in the empirical classification only considers global quantitative information representing an averaged value in an annual timeframe or greater. The description and further processing of those datasets is described below.

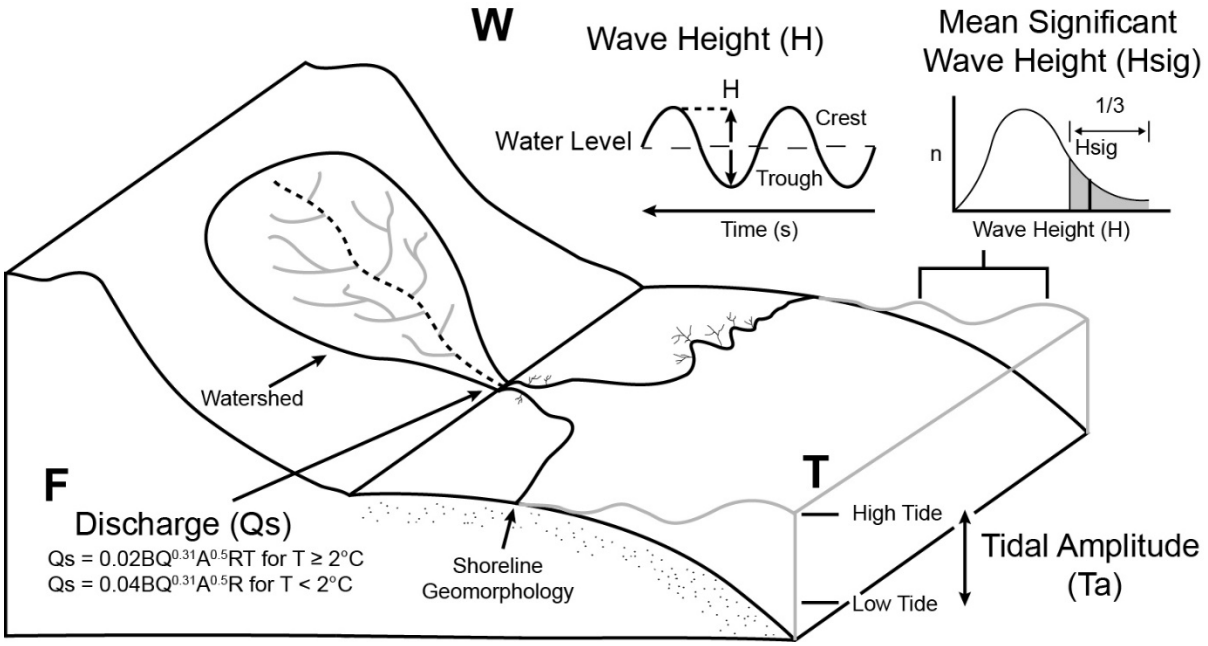

Figure 3. Parameters and datasets used as proxies for the automated ternary process classification (**F, T** and **W**) of a given shoreline section. Fluvial proxy (**F**) is determined from discharge (Qs) based on the area of the watershed, relief, lithology and temperature (see text; Milliman and Syvitski, 2007). Tidal proxy (**T**) is defined by the amplitude for each tidal constitute that combined compose the tidal range. Wave proxy (**W**) is based on mean significant wave height (Hsig) defined as the mean of the

third highest wave heights where a wave height (H) is determined as the height between the trough and crest of a wave.

4.1.1. Mean Significant Wave Height

Mean significant wave height (Hsig) is a measurement of the mean of the third highest wave heights. A wave height is defined as the distance between trough and crest between any given wavelength cycle (Figure 3; Tolman, 2002).

A global dataset of Hsig has been amalgamated from two sources to provide seamless coverage. The first source of data is provided by the National Oceanic and Atmospheric Administration (NOAA)'s WAVEWATCH III program (Tolman, 2002). The mean of over 20,000 hindcast datasets calculated every 3 hours between 2006 and 2013 were combined and provide global coverage including significant regions of the arctic at 0.5 degree resolution (approx. 50km). Though, the Mediterranean, Black Sea, Red Sea and the Persian Gulf are not included in this model. To supplement those regions, the WorldWaves Global Offshore Database developed by Fugro OCEANOR was used. This is an analysis of Hsig between 1997 and 2006 (Mørk et al., 2010). The global dataset is gridded at a 0.5 degree resolution (approx. 50km) based on the European Centre for Medium-range Weather Forecasts (ECMWF) models relying on Topex satellite altimeter data that are subsequently calibrated to global buoys. Hsig used in this study ranges from 0 to 4.4 m.

4.1.2. Tides

Global tidal models have been derived through the Global Tide FES2012 (Carrère et al., 2012) project available through Aviso (Aviso, 2012). This model is based on altimetry datasets in conjunction with improved bathymetry and tidal barotropic equations to provide global coverage at a 1/16 degree resolution to model 32 individual tidal constitutes. Here we use the main diurnal (K_1, O_1) and semi-diurnal (M_2 and S_2, N_2) tidal constitutes to map global

tidal range as $2(K_1 + O_1 + M_2 + S_2 + N_2)$. The global tidal range used in this study varies from 0 to 13.8 m.

4.1.3. Fluvial

There is no global dataset that provides direct information on mean fluvial discharge for all of the world's rivers. These proxies are derived from hydrological models that study the contributing drainage area (watershed) to a sink (pour point) by analyzing digital elevation models (DEM) that reflect its fluvial network. Many studies have proposed basin delineation and global discharge models that reflect that watershed (Milliman and Syvitski, 1992; Vörösmarty et al., 2000b, a; Fekete et al., 2002; Global Runoff Data Centre, 2007; Milliman and Syvitski, 2007). The current study requires a global exoheric analysis of relative fluvial discharge at its fluvial mouth at a resolution that captures the variability of small fluvial rivers that may influence shoreline geomorphology. This is important as it is recognized that small mountainous rivers have significance to the fluvial discharge budget (Milliman and Syvitski, 1992) and thereby by extension modern coastline geomorphology. For this purpose, we feel that existing digitally available basin discharge models (Vörösmarty et al., 2000b, a; Fekete et al., 2002; Global Runoff Data Centre, 2007) are insufficient in capturing those small rivers.

To provide the highest possible fluvial discharge model we use two amalgamated sources to delineate basin watersheds worldwide. A 15-arc second watershed derived from the HydroSHEDS project (Lehner et al., 2008) based on a hydrologically conditioned SRTM digital elevation model (DEM) at a 90 m resolution data between 60 degrees north and south. To supplement this dataset in the northern parts, a 15 arc-second breakline emphasis (a resampled DEM that highlights ridges) of the GMTED2010 DEM dataset (Danielson and Gesch, 2011) was used to calculate watersheds utilizing standard hydrological tools available in ArcGIS (ESRI, 2014). A relative discharge associated with this watershed model followed

the proposed methodology of Milliman and Syvitski (2007) with the assumption that this finer watershed model upscales accordingly. This is based on equation 1;

$$Qs = 0.02BQ^{0.31}A^{0.5}RT \; for \; T \geq 2\,^{\circ}\,C \qquad \text{eq. 1a}$$

$$Qs = 0.04BQ^{0.31}A^{0.5}RT \; for \; T < 2\,^{\circ}\,C \qquad \text{eq. 1b}$$

$$Q = 0.075A^{0.8} \qquad \text{eq. 2}$$

where Qs is discharge in kg/s, B captures information regarding lithology, glacial erosion and anthropogenic conditions, Q is watershed discharge in km^3/yr (eq. 2) , A is watershed area in km^2, R is maximum relief in km and T is mean basin temperature in Celsius. Lithology is based on a systematic analysis of global maps produced by Syvitski and Milliman (2007) showing the distribution of the major 425 basins. Smaller basins were based on the proportion of lithologies (Dürr et al., 2005) within each watershed as defined in Table 1, reflecting the description of lithologies and coefficient used by Syvitski and Milliman (2007). We ignore anthropogenic conditions and ice erosion in our calculation that may attribute an additional 17% to the observed discharge (Milliman and Syvitski, 2007).

Table 1. Lithologies and thresholds used to determine the lithology factor (B) of watersheds. Dominant threshold defines the threshold percentage that the lists of lithology codes compose the lithology of the watershed. Otherwise a default value of 1 is given. Hard rock = Pr, Pb, Pa, Mt, Cl; volcanics = Va and Vb; sedimentary = Ss, Sm Su; carbonates = Cl; Ad = Alluvial

Category	Dürr *et al* (2005) Lithology Code	Dominant Threshold	Lithology Factor
Hard rock acid plutonic or metamorphic rocks	Pr, Pb, Pa, Mt, Cl	> 80% hard rock	0.5
Hard rock but mixed lithology	Pr, Pb, Pa, Mt, Cl	>80% hard rock & > 50% Cl or > 20% hard rock & >10% Vb or	0.75

		Va	
Volcanic, carbonate outcrop or mixed hard/soft lithologies	Va, Vb, Sc, Ad	> 20% volcanics/carbonates & < 35% Ad & < 20% Sm	1
Soft lithologies with significant hard rock lithologies	Ss, Sm, Su, Sc, Ad	50 - 65%	1.5
Predominatley soft lithologies	Ss, Sm, Su, Sc, Ad	> 65%	2

Maximum relief, R, is taken as the highest elevation within its given watershed based on GMTED2010 data at a 15-arc second resolution (Danielson and Gesch, 2011). Mean temperature, T, is taken from MODIS, the annual day-time land surface temperature of 2013 (NASA LP DAAC, 2001). A visual inspection of the resulting distribution of watersheds with high resolution satellite imagery deemed that a discharge (Qs) greater than 5 captured most small fluvial outputs that influenced the morphology of the shoreline relative to the 5km segmentation. For dry hot desert localities defined by a Bwh or Bwk of the Köppen-Geiger classification scheme (Kottek, 2006), a higher threshold of 15 Qs was more appropriate, in particular to exclude such areas as the Skeleton coast of Namibia. The resulting discharge thereby ranges from 5 to ~57,000 kg/s (Amazon delta).

A fluvial mouth has been defined as the drainage point of a watershed basin to a stretch of shoreline or its closest proximity. As a watershed is a tributary function draining to a single point according to its upstream DEM accumulation profile, the distributary character of multiple channels fan from an apex, especially in fluvial dominated systems is not captured. To address this issue, the discharge associated with a single watershed of the world's major river deltas (e.g., Nile) were manually assigned an equal fluvial strength to adjacent fluvial mouths characterized by an individual river and protruding delta lobe. Globally, 6991 fluvial mouths were identified.

4.2. Combining the parameters to classify the shoreline segments

Mean significant wave height (Hsig) is used as the base value. The relative tidal power is corrected by a coefficient, *K*, in equation 3 to correct for its higher amplitude, as noted by Harris et al. (2002). The relationship best suited to represent the relative fluvial influence of a coastline is determined by equation 4 where Qs is the discharge in kg/s and D is the distance along shoreline from the fluvial mouth. This states that the relative fluvial influence decreases at half the cubed rate with distance from its fluvial mouth whereby the minimum distance is greater than 10km. The initial fluvial contact at the shoreline, where D is less than 10km, is given a default distance of 5km as we hypothesis that this initial contact will have a stronger fluvial impact. As multiple fluvial outputs may be insignificant compared to a nearby larger fluvial system, this algorithm will determine the largest relative influence at a particular location according to equation 4 rather than to its closest fluvial output mouth.

$$Tide = TaK \quad \text{eq. 3}$$

$$Fluvial = \frac{1}{2}(Qs/D^3) \; where \; D \; is \geq 10km \quad \text{eq. 4}$$

These function and thresholds were determined after iterative examination of their relative sensitivity above and below those deemed most suitable. This relationship provided a reasonable shoreline type description of ternary process based on visual inspection using high-resolution satellite imagery (see procedures outlined in section 5.2.). However, regional variability associated with depositional versus erosional coastlines and shoreline geomorphology is not considered. This challenge has been addressed below.

4.2.1. Depositional versus erosional

Inman and Nordstrom (1971) used a shoreline nomenclature that separated mountainous and erosional shorelines from depositional shorelines associated with wave and fluvial

deposits. Defining this in the current study is important for two reasons i) the ternary process classification and, ii) when looking for modern analogues for ancient systems.

To separate depositional environments from erosional (rocky) shorelines, a high resolution global lithological map (Hartmann and Moosdorf, 2012) was assigned to the most proximal stretch of coastline whereby waterbodies (wa) or unconsolidated sediments (su) were defined as potentially depositional. This does not however differentiate thin veneers of sediment that may be associated with mountainous rocky shorelines and as such digital elevation models of the world, SRTM (Reuter et al., 2007) and GMTED2010 (Danielson and Gesch, 2011), were used to highlight low lying gradients (<0.8) regions that are above 250km^2 in area. An examination of the difference between the two datasets highlighted on a regional scale, areas that are in net erosion, in particular, the shorelines of eastern Chile off the Andes and many Pacific islands were excluded to produce the final product shown in Figure 4.

The relative tidal influence of equation 3 in relation to those erosional coastlines was found to be significantly less than depositional settings and as such a coefficient of tide * 0.25 is applied. A subcategory of erosional settings, Fjords, as defined by Dürr et al. (2005), were deemed even less tidally influenced, an important distinction to define the particularly Wave-dominated shorelines of the Labrador Sea, offshore Northwestern Canada and Eastern Greenland with a coefficient of tide * 0.15.

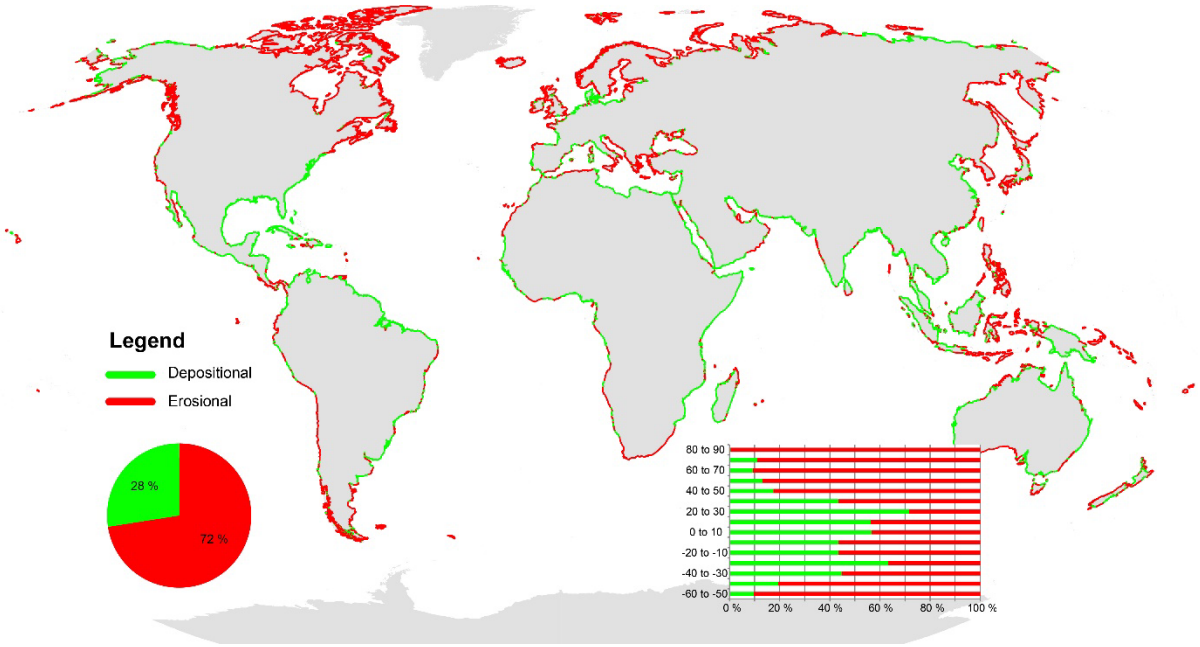

Figure 4. Global classification of shorelines as erosional (rocky) or depositional. Pie chart and a 10 degree binned latitude graph show the proportion and latitude related distribution of erosional versus depositional shorelines.

4.2.2. Geomorphology

In a global study such as the present one, the resolution of data that describes the relative basinal energy components (i.e. tide and wave), may not be able to capture the smaller scale subtleties associated with coastline geomorphology which may locally, significantly modify the relative dominant depositional process. Tidal range is of primary concern as it is not a direct proxy for tidal power (e.g., Dalrymple, 1992; Davis Jr, 2013). Tidal power is measured by a coastlines tidal prism or the volume of water moving through the geomorphology of a coastline within a given timeframe. This is evident in the current global study because the basic relationship of wave height and tidal range alone fail to capture the dynamics of a ternary process relationship. It was therefore necessary to combine information on ternary process proxies (wave height, tidal range and fluvial output) with coastline geomorphology in the absence of more detailed global data series and improved tidal prism information.

Modifications to the various ternary process parameters were assigned based on shoreline geometry. Observations of modern systems indicate that shorelines are more likely to be wave dominated if they are straight and smooth (Davis Jr and Hayes, 1984) and more likely to be tide modified when characterized by highly embayed, rough shorelines with funnel shaped features (Ainsworth et al., 2011). Therefore a measure of the plan view "shoreline roughness" can be used to improve the classification predicted from the purely process based approach.

To measure coastline geomorphology a function of shoreline roughness index, RI, (shoreline length / shortest distance) was used to distinguish relatively smooth shoreline stretches from rough shorelines, Figure 5. Within depositional settings, a very rough shoreline (RI >2) such as many portions of western Florida in the Gulf of Mexico, have a slightly higher tidal influence and therefore the tidal strength is increased by a factor of 1.5. In contrast, extremely straight shorelines (RI <1.15) will have a higher probability of being Wave-dominated and the tidal strength is reduced (tide x 0.6).

Erosional settings that have rough shoreline typology, are not necessarily associated with a higher tidal influence but rather a rocky coastline with erosional inlets (e.g. Mediterranean) that otherwise do not have the ability to rework unconsolidated sediment. Straight shorelines of erosional settings (rocky coastlines) are particularly Wave-dominated, even in macro-tidal settings (e.g., Bahia Grande, Argentina or Sea of Okhotsk, Russia), as are shorelines associated with desert climates (defined here by a dry hot desert climate classification, Bwh or Bwk, of Kottek (2006)), and those regions were assigned a lower tidally influence by a function of tide x 0.25.

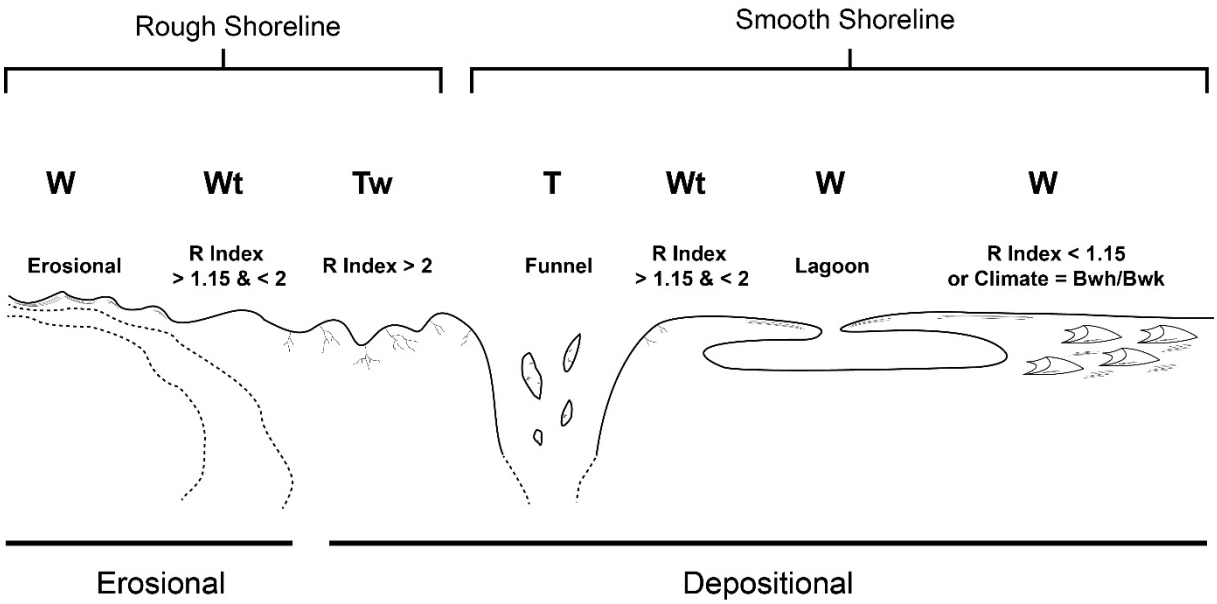

Figure 5. Shows a schematic illustration of the variation of shoreline geomorphology of erosional and depositional settings. Smooth shoreline stretches measured by an RI index less than 1.15 may comprise aeolian, beach ridge and lagoon environments and have a higher probability of wave-dominance (e.g., **Wt** or **W**). In contrast rough shoreline stretches (RI > 2) have a higher probability for tidal modification (e.g., **T** or **Tw**), expect for erosional headland settings. However funnel shaped shoreline geomorphologies may have a smooth shoreline that otherwise are Tide-dominated (**T**).

Funnel shaped shorelines are not captured well by the RI index, for instance the Tide-dominated channels of the Niger delta, Nigeria, Figure 6A, have a relatively smooth shoreline when examining the 5 km coastline segments used in this study, Figure 6B. This piece of shoreline is clearly funneled and tide dominated therefore an alternative modification is required. While it may be possible to define these funnels using an adaptive RI method that would determine the appropriate shoreline length to measure over its shortest path, this was not considered due to the complexity of its implementation on a global scale.

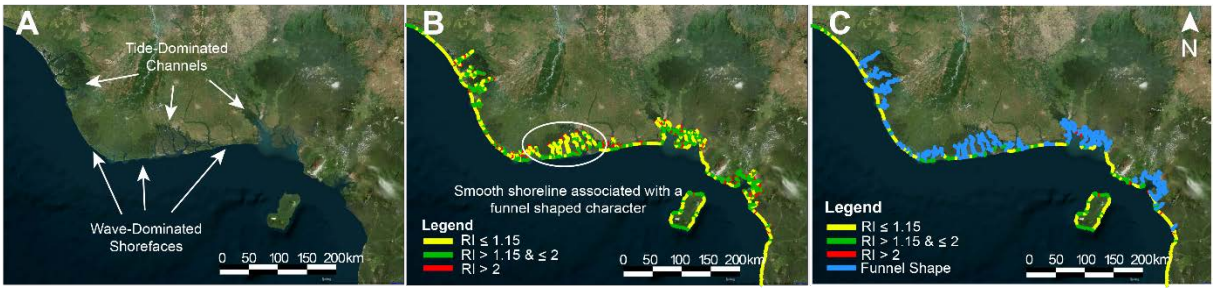

Figure 6. Illustrates the problem arising from the characterization of shoreline geomorphology solely based on the calculation of a shoreline roughness index (RI in Fig. 5). **A** shows satellite imagery of the Niger delta in Nigeria (see Figure 7) which is characterized by a mix of Tide-dominated channels and Wave-dominated shorefaces. **B** shows the calculation of a RI index based on 5 km shoreline segments to identify a significant portion of smooth shorelines within a Tide-dominated funnel shape. One solution is presented in **C** that will define funnel shapes as those sections of shoreline that intrude landwards to create a funnel shape with a perpendicular landmass within 35 km. Imagery from Bing©.

Instead, a funnel shaped stretch of shoreline was determined by an additional algorithm. The first step of this algorithm calculated the seaward direction along a stretch of shoreline as the direction that is not adjacent to a terrestrial landmass (Wessel and Smith, 1996). Once the seaward direction was determined, a second stage measured a 35km perpendicular line to each 5km segment of shoreline and calculated whether that intersected with the same landmass body. If it did, it was assigned as funnel shaped, Figure 6C. It will also register a funnel if the orthogonal landmass to a shoreline is depositional whether that be a strait (e.g. Strait of Malacca) or tidal bars within a larger funnel shape (e.g. Amazon). To ensure that funnels were not registered in enclosed lagoons or fjords, the global definition of Dürr et al. (2011) has been used to eliminate those from consideration. Manual modification to the definition of lagoons was made to correct for its lower dataset resolution (e.g., to separate estuaries of North Eastern USA from their lagoons). The algorithm may classify restricted Wave-dominated bays as partly funnel shaped however the inlet of bays are generally wide which will cause the calculated funnel length to be short, although this is a source of potential

error. Therefore minimal manual editing was performed to address a few of those concerns to produce the map in Figure 7.

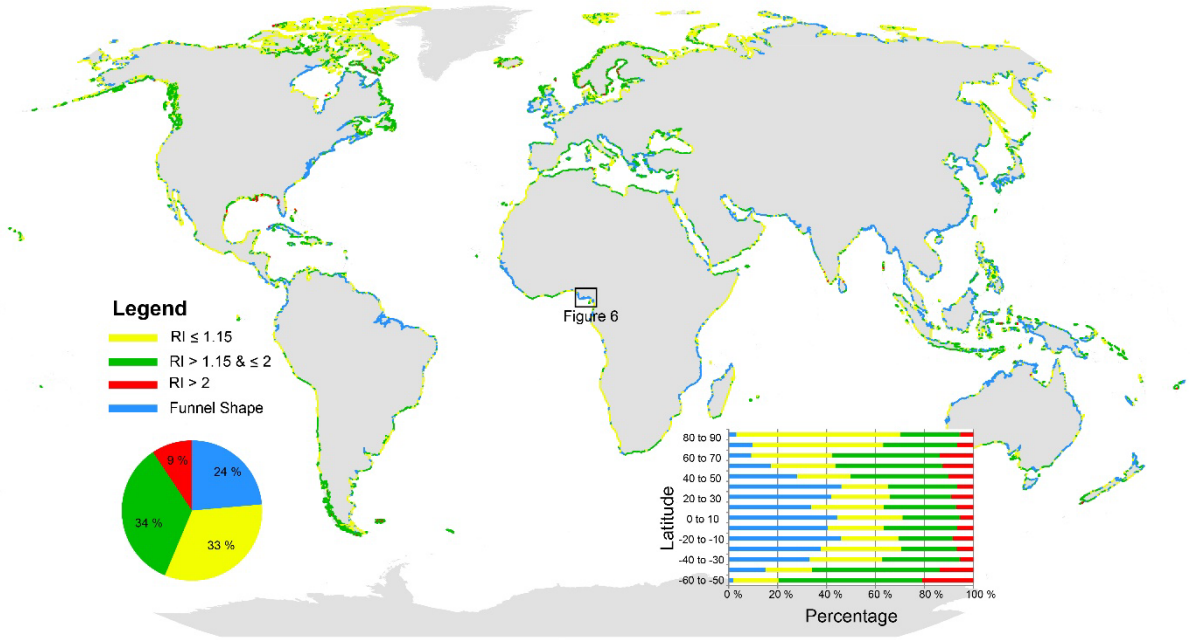

Figure 7. Global shoreline geomorphology displayed with a pie chart and a 10 degree binned latitude graph to show the proportion of RI indices and funnel shaped shorelines. The black box shows the locality of the Niger delta, Nigeria, used in the example for Figure 6.

The relative impact of a funnel shape on the shoreline process dominance was determined by a combination of funnel length and relation to the tidal range. The length of a funnel was determined as the cumulative length that a stretch of shoreline is determined to be within the confines of a funnel shape, while tidal range is split into microtidal (<2m), meso-tidal (2-4m) and macro-tidal (>4m; Davies, 1964). Here we use these as a proxy to relate a relative funnel by its tidal range although we recognize that the geomorphological shape, bathymetry, volume and its relation to tidal prism are not considered. The tidal power is amplified in equation 5 by a funnel geomorphology coefficient (Fg), which is determined by the tidal range and funnel length (Fl) in km. Unlike an RI index, a funnel shape greater than 10km (limit of the shoreline segmentation resolution) can be determined regardless of size.

$Fg = \frac{Fl}{25} if\ Fl \geq 25\ km$ for micro-tidal conditions $(\leq 2m)$ equation 5a

$Fg = \frac{Fl}{15} if\ Fl \geq 15\ km$ for meso-tidal conditions $(> 2 \leq 4m)$ equation 5b

$Fg = \frac{Fl}{10} if\ Fl \geq 10\ km$ for macro-tidal conditions $(> 4m)$ equation 5c

One further consideration is that micro-tidal lagoons (lagoons with a tidal range less than 2 m) were considered to be influenced by minimal tides and thereby a function to the tidal power of tide x = 0.01 was applied (e.g., Gulf of Mexico). By combining the influence of depositional versus erosional shorelines and coastline geomorphology, a set of coefficients have been determined to describe the dominant basinal energy components. The relative influence of those tide and wave components were renormalized to its original basinal energy to ensure that it remained relative to the fluvial component in equation 4.

4.3 Shoreline Classification

Once values of fluvial, tide and wave power have been derived for each 5 km stretch of shoreline their values were evaluated as a percentage of their total and classified according to the two-tier ternary classification scheme described in Figure 1. This entails that any relative ternary process power greater than 70% along a 5km shoreline segment will yield a 1-tier dominated process classification (e.g., F-Dominated, **F**). A relative ternary process power less than 70% will yield a two-tier, dominated and influenced, ternary process classification (e.g., Fluvial-dominated Tide-influenced, **Tf**, Figure 8).

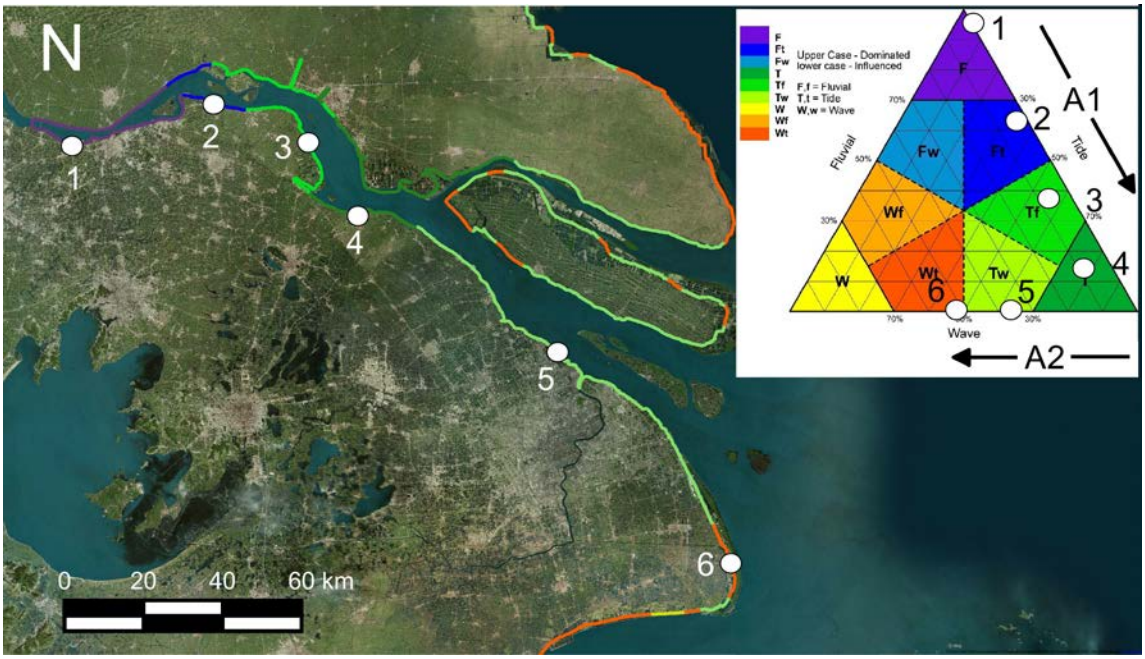

Figure 8. Demonstration of shoreline classification by ternary process along the Tide-dominated Changjiang (Yangtze) delta in China (Hori et al., 2002). Six shoreline localities, numbered 1 through 6, are used to demonstrate the classification of shoreline typology based on its corresponding placement on the inset ternary process classification diagram (from Figure 1) that relates the relative percentages of fluvial, wave and tide power. Line A1 shows a general transition from an initial fluvial signature (> 70% **F** power) to an increasingly Tide-dominated (> 70% **T** power) shoreline (point 1 to 4). Followed by an increasingly wave-modified, open stretch of shoreline, from the Tide-dominated (> 70% **T** power) to Wave-dominated Tide-influenced shoreline (**W** power < 70% and **W** power > **T** power), illustrated by line A2 (point 4 to 6). Imagery provided by Bing©.

The final modification is reserved for small fluvial mouths that were deemed significant in section 4.1.3., though had a discharge too small to be proportionally significant in the proposed classification algorithm, particularly in high energy environments. Thereby, any small fluvial output connected to a shoreline that was not assigned a fluvial classification was assigned as having a fluvial-influenced parameter. These regions are of particular importance in mountainous regions where there are numerous small fluvial input points such as the Andes in South America and eastern portions of Madagascar (e.g., Figure 2h).

5. Results

5.1. Global Distribution

A total of 246,777 segments were classified representing 927,577 km of coastline. These results show that the majority (84%) of the world's coastlines are wave dominated, of which 74% are **W**, 8% **Wt** and 2% **Wf** (Figure 9). Waves are especially important in erosional coastlines and the percentage figures are somewhat skewed because of the irregular geometry of such shorelines exaggerates their global significance. In particular, Fjords, which comprise nearly 41% of the global shoreline length are nearly exclusively within wave dominated environments. Tidal systems make up 16% of the global shorelines; **T**, **Tw** and **Tf** have a relative distribution of 10, 5 and 1 % respectively. Fluvial dominated systems make up <1% of the global shoreline. The global distribution show that most shorelines are wave dominated, including most of South America, southern portions of Australia and Africa, New Zealand, Japan, Eastern Madagascar, Northeastern China and a majority of the Arctic. Tide dominated portions are constrained primarily to the mid latitudes in areas such as northern Australia, Southeast Asia, Indonesia, Malaysia, Papa New Guinea, Brazil, India and West Africa. The major fluvial deltas are associated with major drainage basins on passive continental margins include the Amazon, Irrawaddi, Mississippi, Danube, Ebro, Martaban, Nayarit, Po and the Sao Francisco deltas. Numerous smaller fluvial outputs are distributed throughout the world with notable **Wf** settings on the western coast of South America, Figure 10A and Eastern coast of Madagascar and **Tf** are particularly common around southeast Asia.

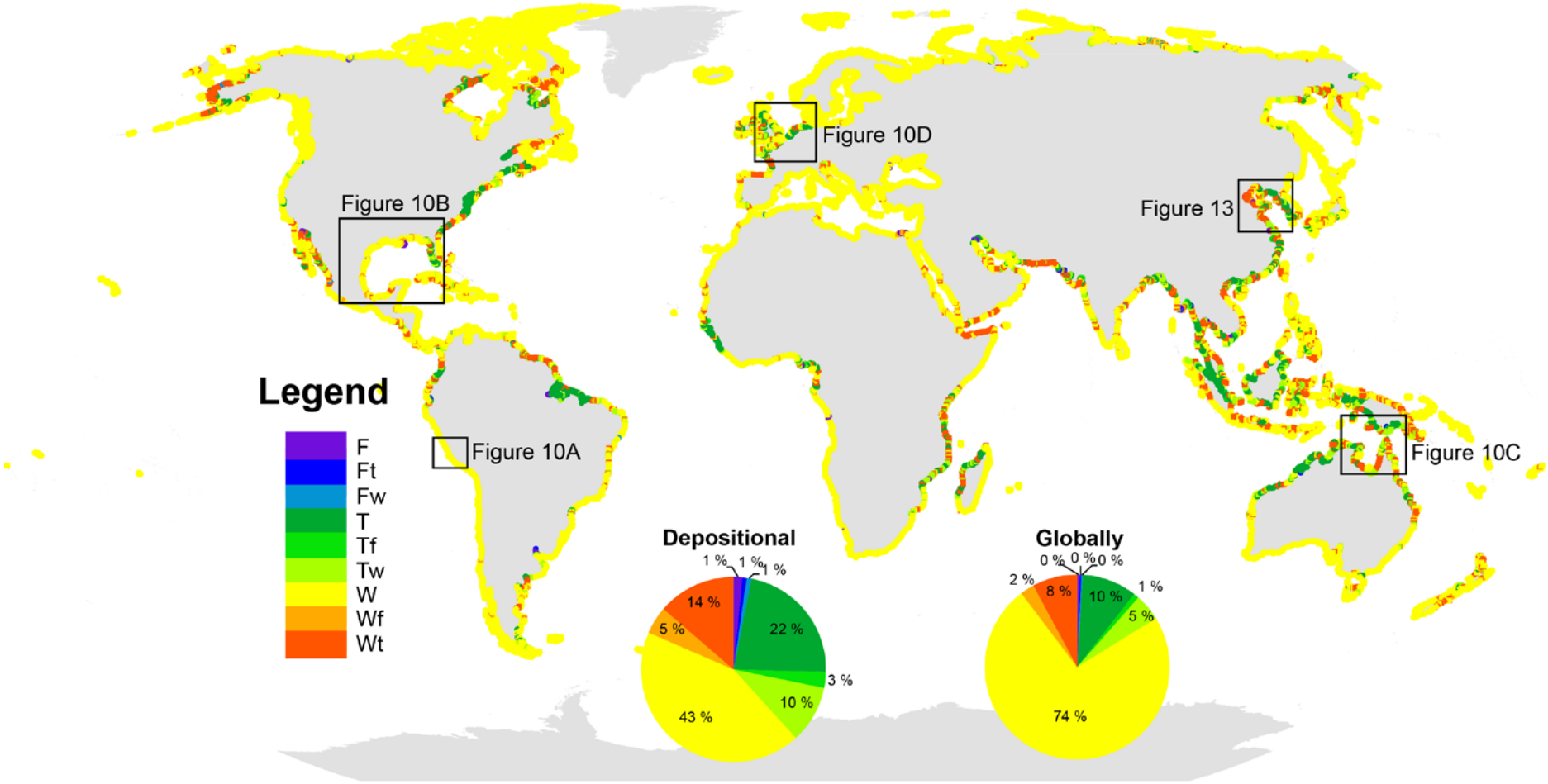

Figure 9. Global two-tier ternary process classification (Fig 1) of modern shorelines. The two pie charts show to the proportion of the ternary process within depositional settings and globally (see Figure 4). Black boxes show the extent used in Figure 10 and Figure 13 to highlight the higher resolution examples of the classification.

Depositional shorelines show a similar distribution to the global shorelines with a majority of wave dominated segments. However the predominance of wave dominated processes (W, Wt and Wf), represent only 62% of the total, while tidal processes increase to 35% and fluvial processes are represented by 3%, Figure 9. The most significant change is the decrease of **W** shorelines by nearly half from 74% to 43% in depositional settings. This decrease in wave processes is related to an increase in **T** shorelines from 10% to 22% and **Tw** shorelines from 5% to 10%. Fluvial conditions are more pronounced with Fluvial-dominated systems (**F**, **Ft**, **Fw**) all increasing above 1%, **Wf** increasing from 2% to 5% and **Tf** systems increasing from 1%to 3% . Figure 10 shows four selected regional examples around the world that represent a variety of different shoreline types.

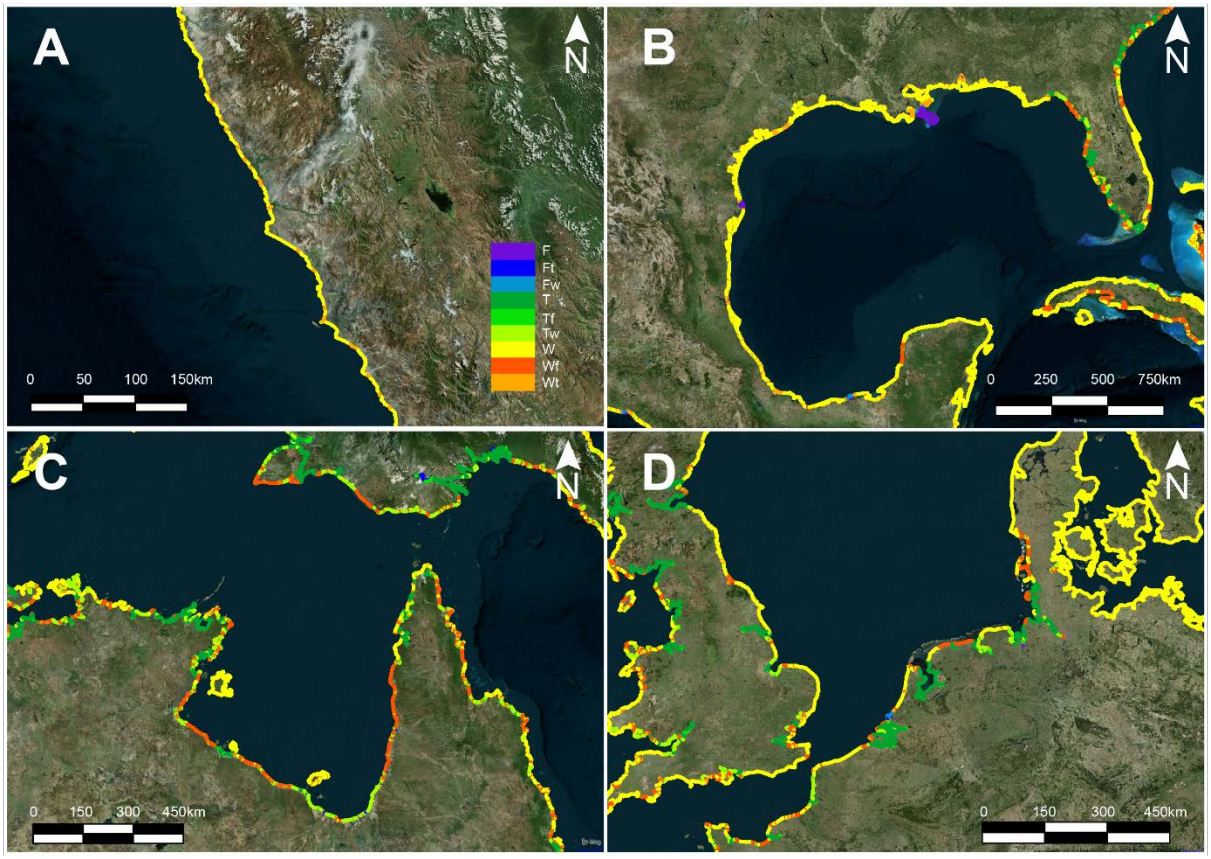

Figure 10. Selective examples of ternary process classification from the insets shown in Figure 9. **A** shows a **W** shoreline with regular fluvial inputs to yield a **Wf** shoreline on the Peruvian coastline in South America. **B** shows a predominately depositional and Wave-dominated coastline in the Gulf of

Mexico with numerous fluvial inputs to create **F** shorelines in the low basinal energy environment such as the Mississippi and Usumacinta - Grijalva delta. **C** shows a mixed-influenced regional scale overview of the Gulf of Carpentaria in northern Australia and eastern Papua New Guinea. The Gulf of Carpentaria is characterized by a transition from a **W** process on its north-eastern margin transiting to a more-mixed influenced and **T** process southwards that develops into a predominately **Wt** environment with embayment's of **T** and **Tw** towards the west. **D** shows an example from Europe to show wave dominated shorelines interweaved by Tide-dominated shorelines and deltas such as the Rhine-Meuse delta. Imagery from Bing©.

5.2. Validation & Quality Control

To validate the accuracy of the proposed classification, 100 points within depositional settings (Figure 11) were chosen at random and manually classified from high resolution satellite imagery based on the geomorphology (e.g., Figure 2) following the modified classification scheme of Ainsworth et al. (2011). The results are summarized in Table 2 to show a correct matrix for the proposed automated classification versus its manual interpretation. Of those localities, 85% were classified correctly by the automated algorithm and an additional 8% identified the dominant process correctly, 7% were identified as partially correct while no classifications were completely wrong within the sampled quality control region.

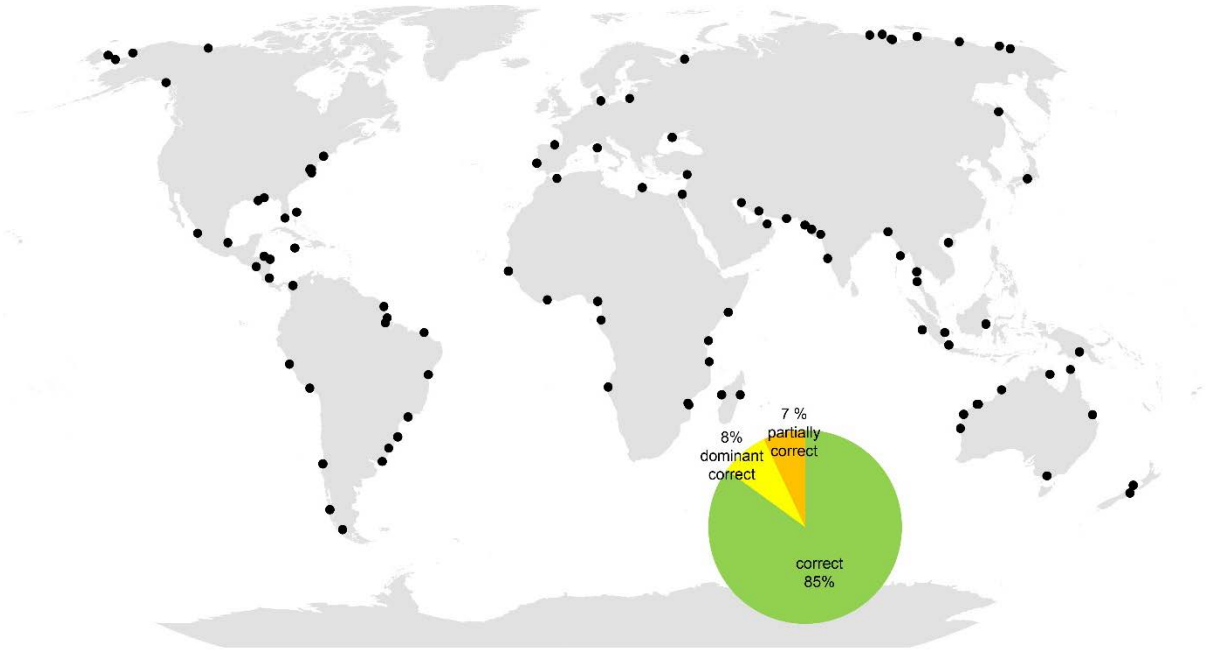

Figure 11. Random selection of 100 samples points used to quality control the automated classification versus a manually assessment (Table 2). A pie chart shows the proportion of those samples where the automated classification is correct, dominant process is correct or partially correct.

Table 2. Shows the number of correct values the automated classification identifies in comparison to a manual interpretation from high-resolution satellite imagery of 100 randomly selected points (Figure 11) on the global shoreline shorelines. Green boxes indicate that the classification was correct, yellow boxes show that the dominant process was correct, orange boxes show that the classification was partially correct and red boxes indicate that the classification was completely wrong.

		Automated Classification								
Manual Interpretation		F	Ft	Fw	T	Tf	Tw	W	Wf	Wt
	F	1								
	Ft	1	1		1					
	Fw			3				1		
	T				20		3			3
	Tf					2				
	Tw				2		5			
	W							42		
	Wf							1	5	1
	Wt				1		1			6

5.2.1. Comparison to previous studies

A comparison of the results gathered in the current study to the manual quantitative analysis by Short (2006) of Australian coastlines is summarized in Figure 12 to show comparable findings both visually (see Figure 14 in Short, 2006) and quantitatively. The southern coastlines of Australia are highly Wave-dominated related to the open-body of water and narrow shelves to create Wave-dominated estuaries, deltas, lagoons and strand-plains. The northeastern coastline shows an increasingly Tide-dominated characteristic although isolated packages of strand-plains and Wave-dominated deltas are found along the rocky shoreline. Towards the northwest, a wide continental shelf promotes a higher tidal influence although Wave-dominated strand-plains are still prominent in this area. Finally the Gulf of Carpentaria in northern Australia has a highly mixed process environment of tide, wave and fluvial processes, Figure 10C.

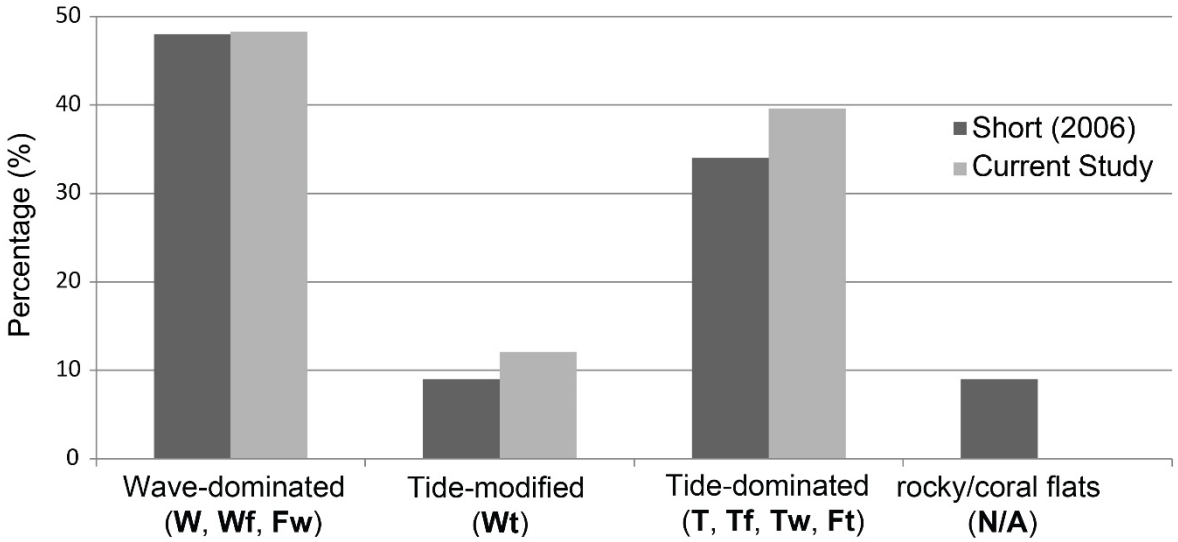

Figure 12. A comparison of the manual shoreline classification of Short (2006) for the Australian coastline and its corresponding automated classification used in this study denoted by bold letters within brackets. Note that the beaches associated with rocky/coral flats category of Short (2006) do not have a corresponding classification in the current study. **F** shorelines that represent less than 1% of Australian coastlines have been excluded.

Expanding the resolution and detail captured around Australia to the global scale and comparing that to the previous global shoreline typology study of Dürr et al. (2011) show some distinct differences. Most notable is that tidal systems of the current study have decreased on a global scale from 22% to 16%.

This can be accounted for in the present study by improved datasets that have been used to capture a better shoreline delineation and regional variability. For instance, the Yellow and Bohai Sea, is represented by a high tidal range however a significant portion of the eastern shoreline is represented by a Wave-dominated coastline that in part is captured by the model here (Figure 13). In general, this region shows that erosional settings are predominately Wave-dominated while tidal influence is restricted within protected embayments and funnels. Mapping the individual fluvial outputs rather than stretches of coastline that contain fluvial output show that fluvial influence may be significantly less at 3% than previously thought (e.g. 32% in Dürr et al. 2011).

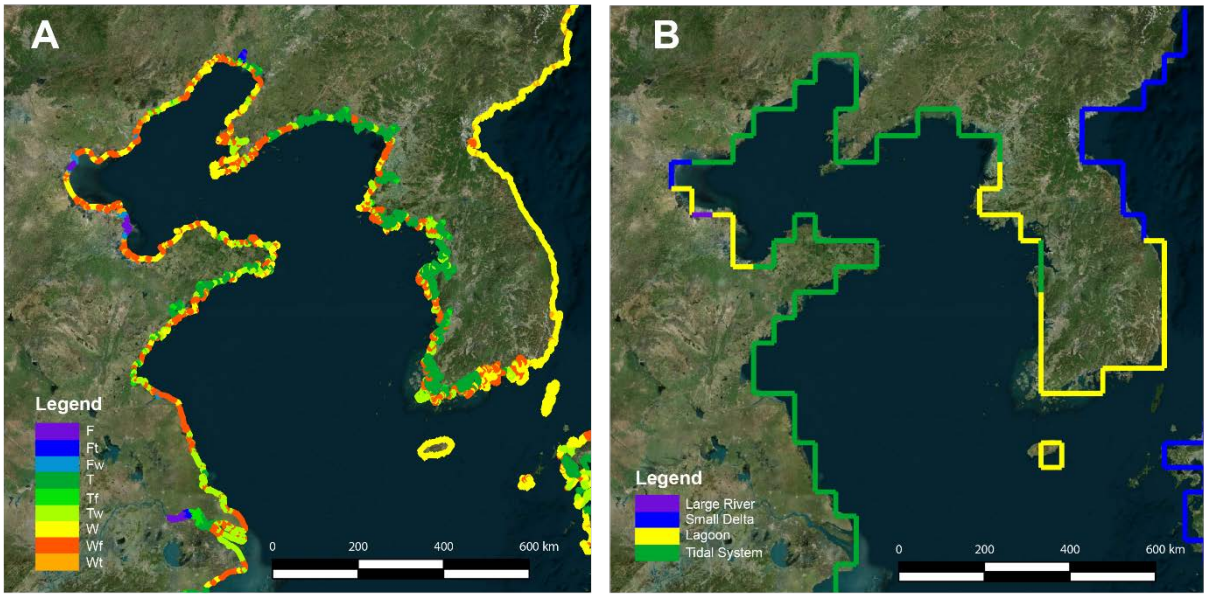

Figure 13. Comparison to previous work in the Yellow/Bohai sea of eastern China and Korea (refer to Figure 9 overview). **A** shows the ternary process classification used in the current study. **B** shows the classification scheme of Dürr et al. (2011) for the same region. Note the discrepancy in resolution and

the added variability captured by the current model. This increased resolution highlights a more Wave-dominated environment, particularly on the eastern shorelines of the Yellow Sea and the Bohai Sea. Imagery provided by Bing©.

5.2.2 Sources for Potential Error

While the overall match between the automated and manual classifications are reasonable (Table 2; Figure 12; Figure 13), it is useful to consider the sources of the errors that are observed. These errors are considered to have arisen for a variety of reasons. Firstly, the resolution of the data that were used to construct the classifications is significantly lower than the subsequent classification. The wave power (mean significant wave height) has a gridded resolution of approximately a 50 km (0.5 degrees) and the tidal data is gridded at every 6 km (1/16 degrees). Both datasets typically model offshore oceanic conditions well but are less accurate in shallow conditions. These were then used to classify the coastline into 5 km intervals. It is therefore possible that detail is lost.

With a lack of global tidal prism data, a combined dataset of tidal range, coastline geomorphology and lithology has provided a proxy for relative tidal power. Tidal prism data could improve a tidal power parameter and reduce error in future quantitative ternary process classifications given that the accuracy and resolution of such data is obtained at a resolution that is able to capture subtle coastline geomorphologies.

Data for watersheds and fluvial output is generated from a delineation of drain basin area from a global digital elevation models (DEM) and uses empirically derived relationships to determine output and delta mouths, this is also a potential source of error. A further source of error in the fluvial portion of the input is that the output from a fluvial system at the river mouth is assigned to a single node which in larger deltas, with distributary patterns on the delta plain may reduce the wider spread of fluvial influence along the coastline. Finally the

results of the algorithm are also heavily influenced by shoreline morphology and shoreline lithology delineation as defined by Wessel and Smith (1996) and Hartmann and Moosdorf (2012), respectively, which may propagate into the classification present herein.

A majority of errors occur on shorelines that are sensitive to tide and wave power variability where global dataset proxies for ternary process have failed to capture the subtleties and importance of seasonal basinal energy changes. While the classification is not perfect and there is considerable potential for error we feel that the accuracy presented here appropriately defines ternary process on a global scale with an element of regional variability to a level that is useful and can shed light on the global controls on shoreline type.

6. Correlation and causation; controls on shoreline geometry

Figure 9 shows the global distribution of shorelines by ternary process, highlighting the relative proportions on global shorelines and on shorelines that are depositional. In the following section we attempt to investigate this distribution by correlating it against a series of parameters that are traditionally thought to exert some control on shoreline systems. These include latitude, shelf width, tectonic basin type and climate. Whilst correlation does not always imply causation, the results shed interesting light on the relative importance of these factors.

6.1. Latitude

The relative proportions of the 9 process classes were analyzed in 10 degree latitude bins (Figure 14). Results show that the equatorial and mid latitude regions show a more mixed process environment (**T**, **Tf**, **Tw**, **F** and **Ft**) which passes to greater wave dominance at higher latitudes. A similar bell-shaped profile is shown for **Wf** and **Wt** which are more common around the equatorial and mid-latitudes in comparison to higher latitude regions. This is a

reflection of the distribution of depositional shorelines at present (see Figure 4), which are concentrated around the equatorial and mid-latitudes.

Plotting the basinal energy (combined tide and wave) by latitude shows a general decrease towards the northern hemisphere, with the exception of a significant peak around 50 and 60 degrees latitude (Figure 15A; B). This overall northward decrease in basinal energy mirrors the proportion of land versus ocean by latitude which shows the opposite trend (Figure 15C) suggesting that basinal energy is greater where there are large open bodies of water. This trend drastically changes at approximately 60 degrees North as basinal energy peaks in correspondence to the highest proportion of land (over 70% between 60 and 70 degrees North). This would suggest that the configuration of continents today acts as a funnel constricting the strongest tides and waves around the Labrador Sea offshore Greenland and Bering Sea/Gulf of Alaska. This may restrict a significant proportion of tidal resonance from the arctic which makes it difficult for large tides to propagate while recent sea-ice loss may be increasing wave-action in those settings (Overeem et al., 2011). The energy environment is largely controlled by the tectonic plate distribution of the present day.

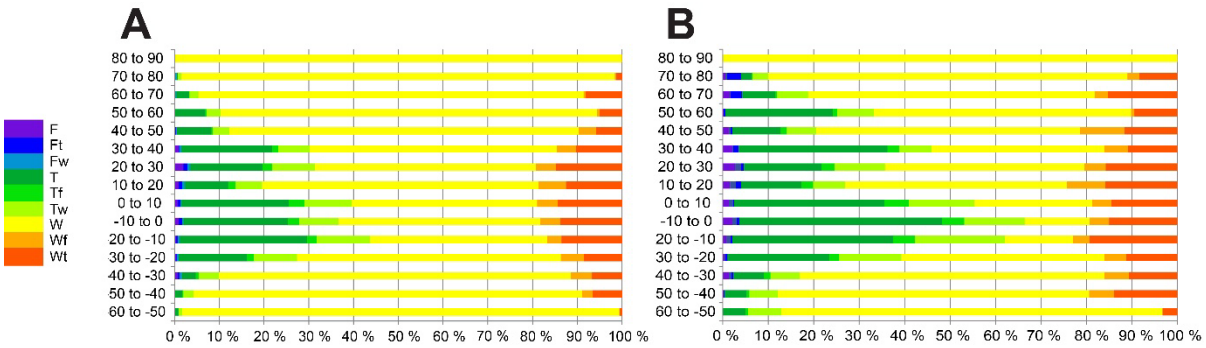

Figure 14. **A** shows the global distribution of ternary process in 10 degree latitude bins. **B** shows the distribution of ternary process in 10 degree latitude bins for depositional shorelines. Both graphs show that the distributions of mixed-process environments (fluvial, tide and wave) are centered on mid- and equatorial-latitudes whereas Wave-dominated shorelines increase towards the poles. Depositional

settings are more mixed-influenced but otherwise show a similar profile to the global distribution.

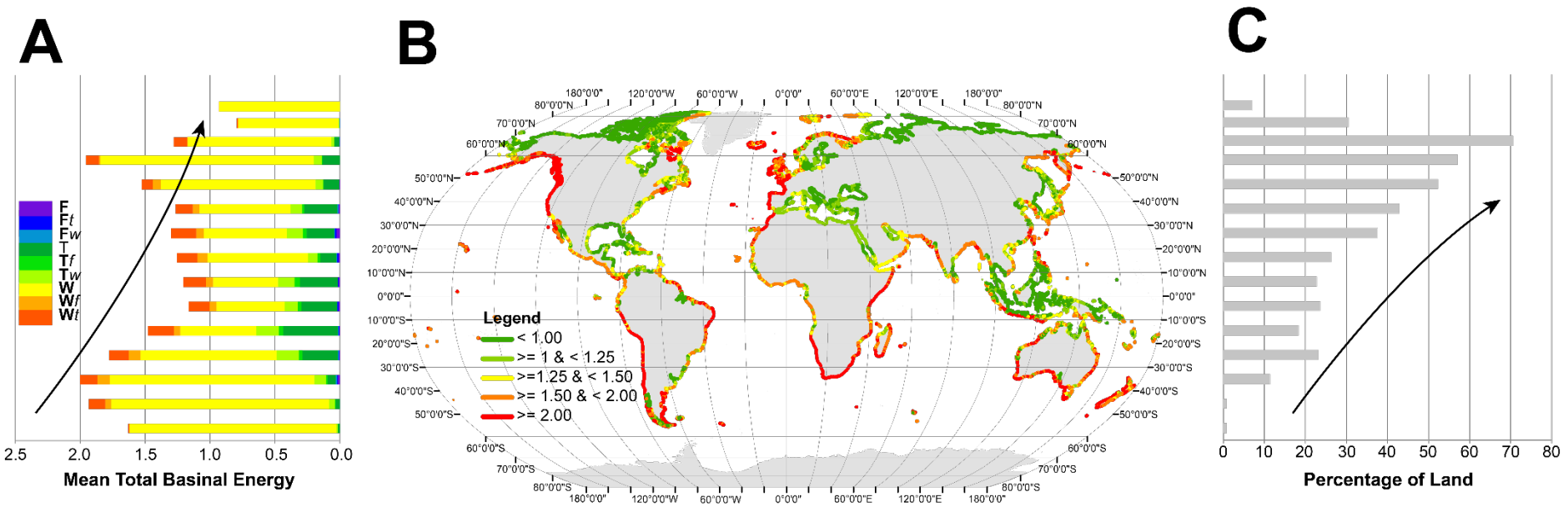

Figure 15 – The relationship between basinal energy and landmass by latitude. **A** the mean total basinal energy (tide and wave) by latitude overlain by the ternary process in Figure 14A. **B** the global shorelines classified by mean basinal energy. **C** the percentage of land by latitude corresponding to the map in **B**. The plots suggests a general decrease in basinal energy while a contrasting increase in the proportion of land versus water towards the northern hemisphere.

6.2. Fluvial Distribution

An analysis on the distribution of fluvial outputs shows the majority occur around the equatorial and mid-latitudes (Fig 15). Given that fluvial discharge is largely controlled by the amount of precipitation (Milliman and Syvitski, 2007), it is not surprising that the most fluvial influence at the shorelines occurs in the tropical latitudes where rainfall is greatest (Fig. 15A). Over 60% of the fluvial outputs in this study were found to be along coastlines that are in net deposition. The proportion of fluvial outputs on depositional versus erosional coastlines by latitude (Fig 15B) does not suggest any particular relationship. This would indicate that any large fluvial output regardless of latitude will be within a depositional setting. The marked decrease between 50 and 60N observed in the proportion of fluvial mouths within depositional settings is attributed to the mainly erosional shoreline of the Sea of Okhotsk that has a significant number of small fluvial outlets (Figure 16B).

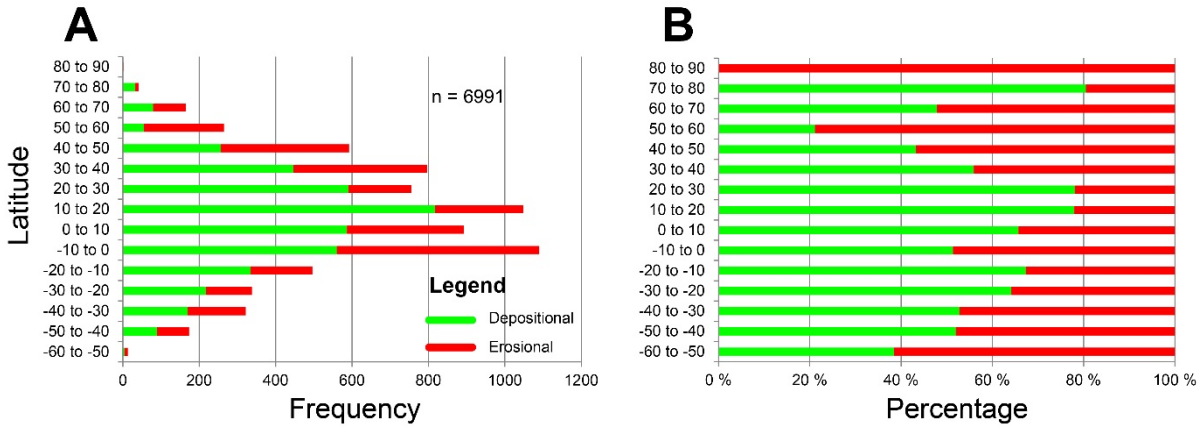

Figure 16. **A**, the frequency of fluvial outputs by 10 degree latitude bins and overlain by the proportion of depositional versus erosional settings. **B** highlights the percentage of fluvial outputs within depositional versus erosional settings binned by 10 degree latitude bins.

The distribution of different types of fluvial dominated and influenced shorelines (**F, Fw, Ft, Wf** and **Tf**) is summarized in Figure 17. Tide-modified fluvial outputs (Figure 17A) are more common in comparison to the proportions of tides globally (Figure 9). This may reflect

that most fluvial outputs occur around the mid latitudes (Figure 17A) and that depositional, more mixed influenced systems also occur in those localities (Figure 4). Wave-dominated fluvial outputs remain the most predominant type of fluvial-modified shorelines. An examination of the strongest basinal energy associated with each fluvial output (tide or wave) binned by a log function its fluvial discharge (1 to >10000 kg/s), Figure 17B, shows that the majority of the largest rivers are Tide-dominated. In contrast, smaller fluvial outputs are more frequent (Figure 17B) and are often Wave-dominated (e.g., Red Sea, Andes). A decrease in tide modified fluvial conditions between 1000 and 10000kg/s is a reflection of a few of the high-energy discharge fluvial outputs off the Andes coastline that are Wave-dominated. Within depositional settings (Figure 17C) tidal systems increase with **Tf** processes by 7% and **Ft** by 2% whereas **Wf** environments decrease by 11% and **Fw** systems remain constant at 4%. This increased tidal-modification is observed in the lower energy fluvial systems (Qs < 1000) of depositional coastline (Figure 17D) considering that higher discharge fluvial settings on a global scale are already predominately within depositional settings.

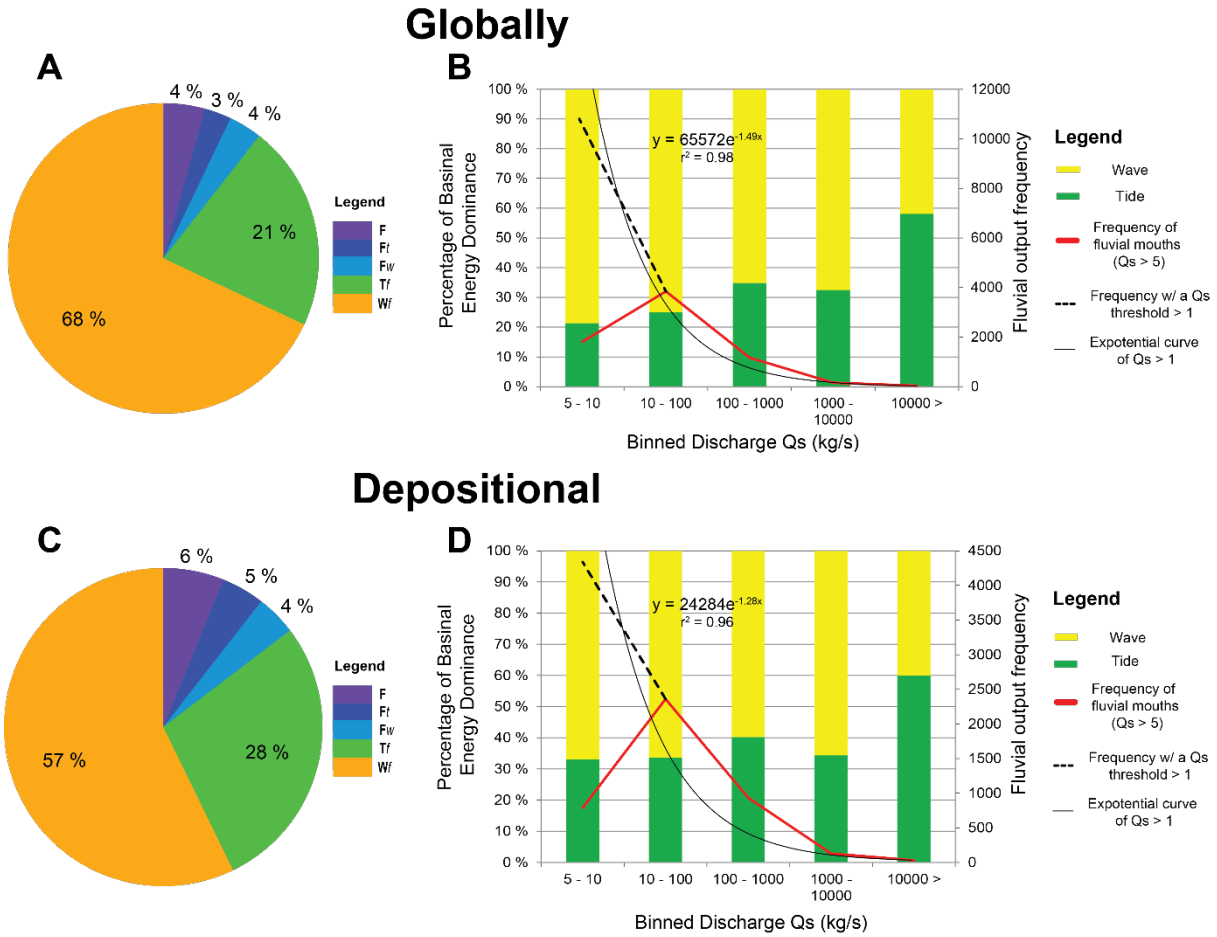

Figure 17. **A** and **C** show the proportion of fluvial processes (**F**, **Ft**, **Fw**, **Tf** and **Wf**) on global and depositional shorelines, respectively. **B** and **D** portray the proportion of dominant basinal energy (tide or wave) of those fluvial processes binned by a log scale of fluvial discharge, globally and depositional, respectively. Overlain on those plots is the frequency of fluvial outputs highlighted by a red line with a Qs threshold greater than 5 as used in Section 4.1.3. Extending the fluvial frequency with a cutoff at Qs > 1 to be consistent with the log scale bins is shown by a dotted black line along with its associated exponential curve fit by a solid black line.

Plots 16B and D, show the frequency of fluvial outputs within bins of fluvial discharge. The results show that most fluvial sources in lower discharge environments are Wave-dominated whereas higher discharge environments are increasing Tide-dominated. As the lowest threshold deemed significant for a fluvial output to a 5 km stretch of shoreline was set at Qs > 5 in section 4.1.3, a decrease in the frequency is shown for the lowest bin. Expanding

the Qs threshold to 1, to be consistent with the log binned fluvial discharge (Figure 17B; Figure 17D), illustrates the evident higher frequency of fluvial outputs from small mountainous rivers in erosional settings (Figure 17B) than depositional settings (Figure 17D). This would suggest that fluvial outputs on depositional settings are less likely to be wave modified and increasingly tide dominated with higher discharge fluvial environments in comparison to erosional surfaces.

A measurement of a watershed's maximum fluvial network length versus its watershed area (above 500 km^2; Figure 18) shows a strong power law relationship, supporting the findings of Vörösmarty et al. (2000b) which suggests that watersheds increase in area with increasing length. As a watershed area is a strong component in fluvial sediment discharge in equation 1 (Milliman and Syvitski, 1992; Milliman and Syvitski, 2007), that information may be a useful indicator in palaeo-reconstructions to predict fluvial size by combing it with other assumptions on lithology, maximum relief and climate.

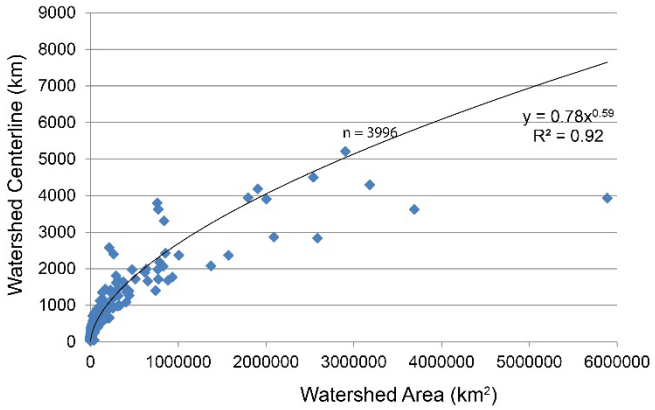

Figure 18 (left). The centerline length of a watershed versus its area in km^2 for watersheds with an area greater than 500 km^2. The centerline length of a watershed is a measurement of the longest upstream river network length from its fluvial mouth.

6.3. Shelf Width

The influence of continental shelf width on tidal amplification has been documented for

several decades (Cram, 1979; Clarke and Battisti, 1981; Longhitano et al., 2012). Most recently (Ainsworth et al., 2011) linked the occurrence of wide shelves with increased tidal influence at the shoreline and conversely suggested that narrow shelves favored the development of more wave dominated systems. To test and quantify this relationship a calculation of shelf width was made, based on a shorelines proximity to the continental slope as defined by its 140 m bathymetry mark by Menot et al. (2010).

The threshold for a wide continental shelf was defined by Inman and Nordstrom (1971) as 50 km while Ainsworth et al. (2011) classified this boundary at 75 km. The definition of Ainsworth et al. (2011) was followed in this publication but further subdivided into narrow (≤25km), medium (>25km and ≤ 75km) and wide shelves (>75km) including a separate miscellaneous class for epicontinental seaways (Figure 19) which were manually added as those stretches of shoreline that are not parallel to a continental slope boundary.

Within depositional settings wider shelves are more prominent at 42% and narrow shelves least common at 19% compared to a global distribution where wide shelves are 28% and narrow shelves 26%.

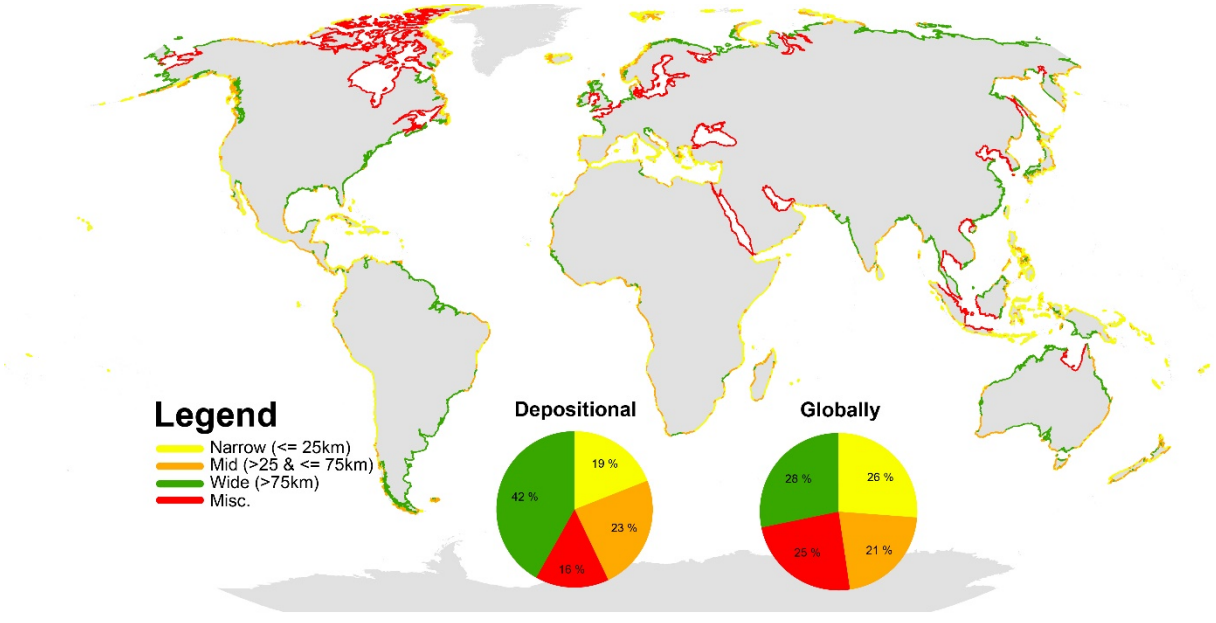

Figure 19. The global distribution of shorelines by binned categories of shelf width. Two pie charts are shown to relate shelf width within depositional settings and globally (see Figure 4).

Results illustrate that an increase in shelf width is associated with an increase in tidal influence at the shoreline, (Figure 20). Tidal processes are related to wider shelves on all shorelines (erosive and depositional) however this relationship is much greater in depositional shorelines (Figure 20B). On a global scale, narrow shelves are strongly wave modified at over 90% and tides less than 5% whereas a wide shelf increased tides to over 30%. Within depositional settings, tide dominated shorelines increase from less than 20% of narrow shelves to >50% on wide shelves. Wider shelves are also more prone to tidal modification of fluvial systems (**Tf** and **Ft)** whereas narrow shelves show a higher proportion of wave modified fluvial systems **(Wf)**. In general mid and wider shelves are more fluvial influenced.

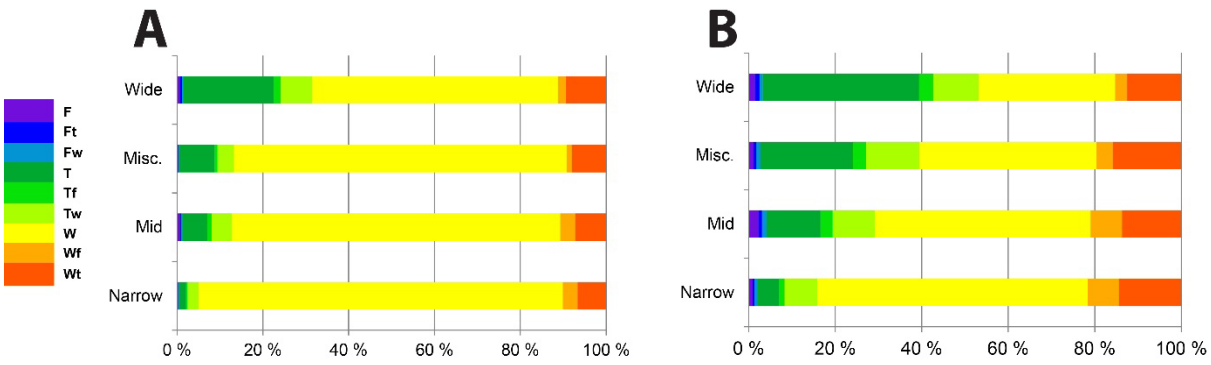

Figure 20. Plots showing the relationship between binned shelf widths in Figure 19 with ternary process in Figure 9. **A** the ternary process distribution by shelf width globally. **B** the ternary process distribution in depositional regions.

6.4. Tectonic Distribution

A combination of tectonic plate distribution (Bird, 2003), stress maps (Zoback, 1992; Sperner et al., 2003) and documented modern distributions (Ingersoll, 2012; Nyberg and Howell, 2015) were used to classify the shorelines into six broad tectonic basin categories:

foreland; fore-arc; passive margin; intracratonic; extensional or strike-slip (Fig 20). The aim here is not provide the same level of detail as the process classification but a generalized global overview of tectonic regimes of shorelines. While an erosional coastline may not be associated with the tectonics of a terrestrial sedimentary basin, its link to a continental shelf provide a reasonable definition.

Globally, intracratonic and passive margins represent over half of all shorelines, fore-arc are at 18% and foreland basins represent 14% whereas extensional and strike-slip basins are less than 4% combined. Similarly passive margins and intracratonic settings are potentially the most significant of depositional settings although foreland basins are twice as prevalent at 20% in comparison to 10% of fore-arc basins. In addition, extensional and strike-slip regimes appear to be more common within depositional settings than erosional shorelines.

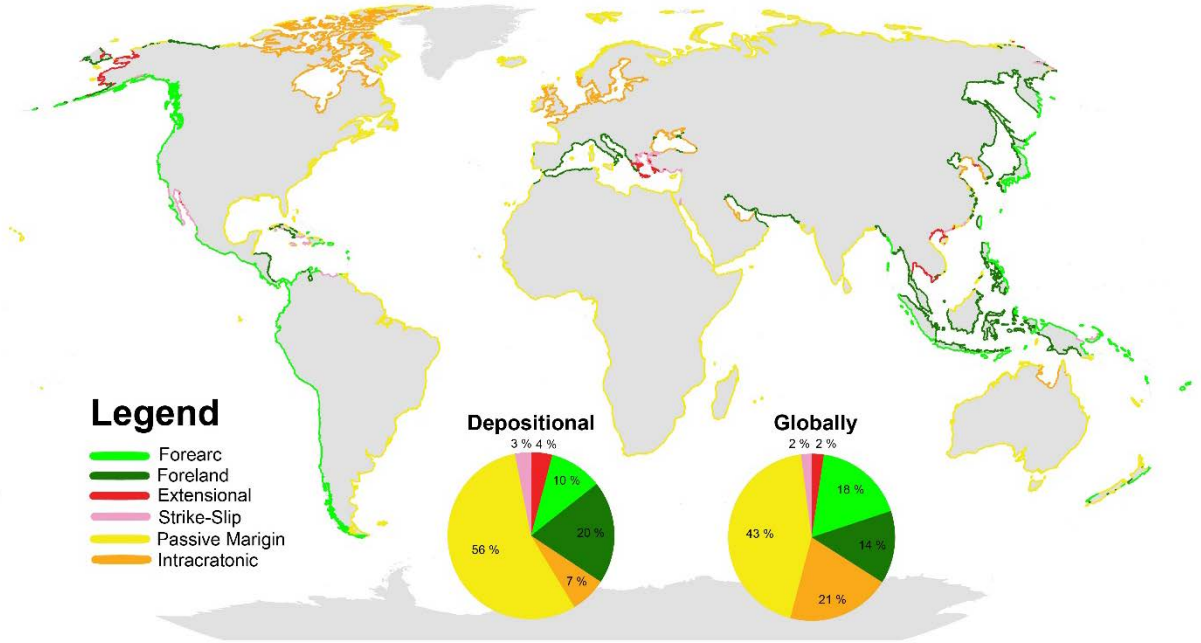

Figure 21. Global distribution of shorelines by tectonic classification. Two pie charts are shown to relate the tectonics within depositional settings and globally (see Figure 4).

6.4.1. Ternary Process and Tectonics

Figure 22 shows the distribution of ternary process by tectonics within areas of net shoreline deposition. Fore-arc basins are the most Wave-dominated environments while foreland, extensional and strike-slip basins are the most tidally-influenced settings. Passive margins are typically wave dominated but show a significant tidal influence. Intracratonic settings are even more wave dominated although this partially because much of the Black Sea is included in this definition. Examining the proportion of those processes related with each basin type, Figure 22B, highlights this relationship further. Tidal systems associated with a fluvial input (**Ft**,**Tf**) are typically found within foreland basins. **F**, **Fw**, **T**, **Tw**, **W**, **Wf** and **Wt** systems are otherwise more common on passive margins and the wave-modified elements of **W**, **Wt** and **Wf** are increasingly significant on fore-arc basins. Extensional and strike-slip settings that are otherwise of a low sample representation have a significant mixed-influenced process including **Ft**, **Tw** and **Wt**.

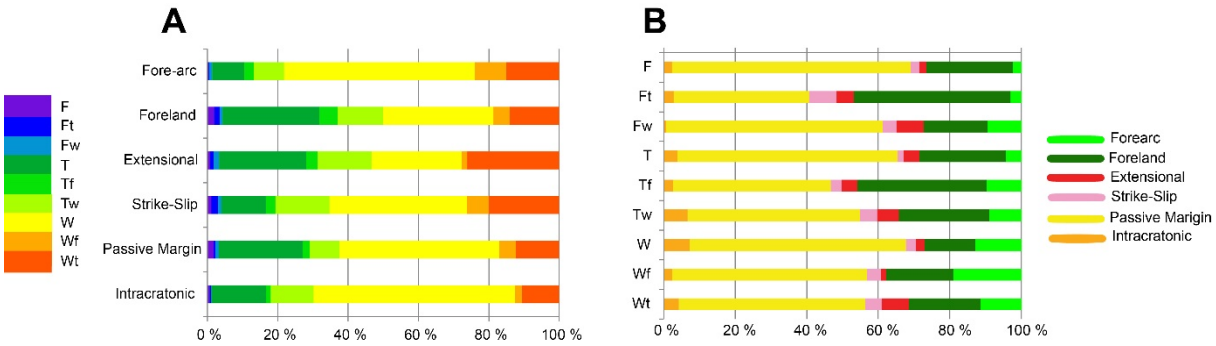

Figure 22. Plots comparing tectonics versus ternary process distribution within depositional settings. **A** plots the ternary process distribution by tectonic setting while **B** shows the tectonic distribution by ternary process.

6.4.2. Climate and Tectonics

An examination of climate (Kottek, 2006) by tectonic regime, Table 3, has shown in particular that most tectonic settings are within equatorial, warm temperate and arid

conditions. Snow and polar conditions are mainly constrained to passive margins, foreland or fore-arc basins. Passive margins are the most dominant within equatorial and warm-temperate climates followed by foreland basins in equatorial settings. Extensional basins are a mere 4% and are constrained primarily to extensional basins of Alaska and Southeast Asia whereas strike-slip basins are even fewer although some may be associated with the Mediterranean. Most fore-arc basins are within equatorial conditions.

Table 3 - Tectonic Setting and Climate of Depositional Shorelines

	Foreland	Fore-arc	Strike-Slip	Extensional	Intracratonic	Passive Margin	Total
Arid	2	2	1	0	1	9	15
Equatorial	11	5	1	1	1	23	43
Temperate	3	2	1	1	4	16	27
Snow	2	1	0	2	1	6	10
Polar	1	1	0	0	0	2	5
Total	20	10	3	4	7	56	100

6.4.3. Shelf Width and Tectonics

Mapping shelf width versus tectonics show that extensional, strike-slip, intracratonic and passive margins are generally associated within epicontinental seaways or wide shelves, Table 4. Most significantly, over half of passive margins and extensional settings are on wide continental shelves. In contrast most fore-arc basins are of narrow or mid width shelves. Foreland basins also have a relatively high proportion of basins within epicontinental seaways (5%) or wide shelves (7%) whereas strike-slip settings are evenly distributed among narrow, mid and wide at 1%.

Table 4 - Tectonic Setting and Shelf Width of Depositional Shorelines

	Foreland	Fore-arc	Strike-Slip	Extensional	Intracratonic	Passive Margin	Total
Narrow	3	4	1	0	0	10	18
Mid	5	4	1	0	0	14	24
Misc.	5	0	0	2	5	3	16
Wide	7	2	1	2	1	29	42
Total	20	10	3	4	7	56	100

7. Discussion

This study illustrates that shoreline typology by ternary process can be classified on a global scale using publically available data on mean significant wave height, tidal range, and calculated fluvial discharge. The results indicate however, that process dominance cannot be predicted by those parameters alone and shoreline geomorphology and erosional versus depositional shoreline regions is a significant component.

Mapping modern shoreline geometry is important for three principal reasons. Firstly, mapping and understanding modern systems have implications for identifying and quantifying the fundamental controls on shoreline type (Boyd et al. 2006) which in turn maybe useful to predict shoreline type in ancient systems. Given that shallow marine shoreline type has a fundamental impact on reservoir behavior, predicting it is highly desirable from a hydrocarbon exploration perspective.

Secondly, modern systems are commonly used as analogs for ancient systems (Tye, 2004; Weissmann et al., 2010; Ainsworth et al., 2011; Howell et al., 2014). Suitable analogues remains a key challenge, which can be easily addressed once global mapping has been undertaken. This is especially important from a hydrocarbon production scenario when analogues will be used to derive geometries and dimensions for reservoir models (Tye, 2004;

Nanson et al., 2012). Finally, a global mapping of shoreline typology has application beyond the hydrocarbon industry in numerous areas of coastal management. These applications are beyond the scope of this discussion but it is considered that the data and methods presented here, could be widely applied.

The analysis of the global distribution of modern shorelines described above suggests that basin morphology, shelf width, latitude, tectonics and climate are key factors that control shoreline typology. These and other controlling factors are interlinked in a complex web of interdependency (Figure 23). Plate tectonics is the first order control which in turn control the other parameters. The following discussion attempts to address the role and interplay between some of these factors in a way that is predictive for hydrocarbon exploration.

Plate tectonics is the continental drift of the Earth's tectonic plates, generating orogenic belts, sedimentary basins and new oceanic floor (Dickinson, 1974). The horizontal and vertical movement of the plates controls the tectonic setting at the coastline, which in turn, influences the shelf width. It also controls the size of fluvial drainage basins and the volumes of sediment supplied to a portion of coastline which is typically much greater on passive margins, draining major continental land masses, than in tectonically active settings. Plate tectonics controls the distribution of sedimentary basins and the creation and destruction of accommodation. It also controls the latitude of the palaeogeographic setting which in turn controls the climate at the shoreline. Finally plate tectonics controls the configuration of the continents and oceans which is a fundamental control on wave energy.

Likewise, base-level controls shelf width. During lowstand times there are narrower shelves which typically increase the proportion of Wave-dominated shorelines until progradational systems on the shelf edge create wider constructional shelves or base-level rises (Figure 23A). During transgressive and highstand times there will typically be an

increase in Tidal-dominated shorelines by amplifying tides on wider shelves (Figure 19; Cram, 1979; Clarke and Battisti, 1981; Ainsworth et al. 2011; Longhitano et al., 2012) until progradational systems build on the continental shelves to narrow shelf width or base-level falls (Figure 23A). Falling base-level may also increase tidal attenuation depending on shelf incisions increased tidal amplification or a shallowing seaways increased tidal current constrictions (Longhitano et al., 2012).

Climate is mainly controlled by latitude and the distribution of the continental land masses by plate tectonics which in turn control the distribution of major ocean and air currents, heat transfer, orogenic effects and geochemical cycles (Hay, 1996). Climate, both at the coastline and in the hinter land influences sediment delivery to the shoreline and also the degree of wave activity. Longer term climatic change at high latitudes leads to glaciation cutting fjords and glacial retreat causing isostatic rebound, which removes significant amounts of high latitude accommodation. Climate also controls weathering and erosion with higher volumes of clay being derived from tropical source areas.

Tectonic setting, which is a function of plate tectonics, is the key control on the nature and rates of accommodation creation (Dickinson, 1974; Van Wagoner et al., 1990) and are also a major control on sediment supply to the shoreline (Milliman and Syvitski, 1992).

Large progradational systems where sediment supply exceeds accommodation, create low-gradient typologies. The channels of those vast low gradient settings are subsequently susceptible to tidal amplification and modification. The majority of the world's largest deltas occur on passive margins, foreland and intracratonic settings and are tidally-modified (Figure 17B and Figure 17D) except in restricted low basinal energy environments (e.g., Gulf of Mexico, Mediterranean and Black Sea). Their distribution, primarily within equatorial to mid-latitudes (Figure 16A) where basins are large and sediment yield high, is controlled by the

current configuration of plate tectonics that govern climate and sedimentary basin geometry (Figure 23A; Milliman and Syvitski, 1992).

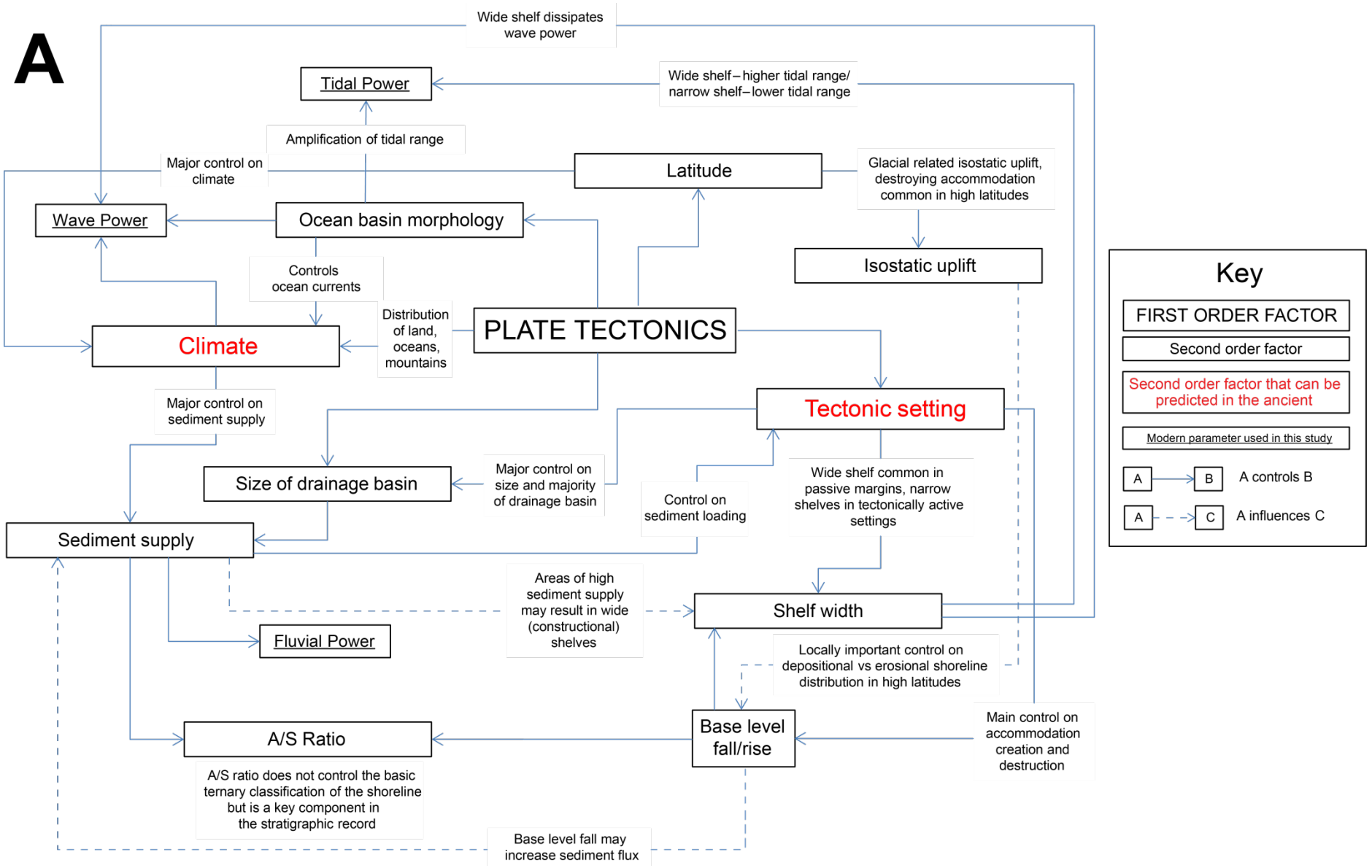
A
Wide shelf dissipates wave power
Tidal Power
Wide shelf – higher tidal range/ narrow shelf – lower tidal range
Amplification of tidal range
Major control on climate
Latitude
Glacial related isostatic uplift, destroying accommodation common in high latitudes
Wave Power
Ocean basin morphology
Isostatic uplift
Controls ocean currents
Distribution of land, oceans, mountains
PLATE TECTONICS
Climate
Major control on sediment supply
Tectonic setting
Size of drainage basin
Major control on size and majority of drainage basin
Control on sediment loading
Wide shelf common in passive margins, narrow shelves in tectonically active settings
Sediment supply
Areas of high sediment supply may result in wide (constructional) shelves
Shelf width
Fluvial Power
Locally important control on depositional vs erosional shoreline distribution in high latitudes
Base level fall/rise
Main control on accommodation creation and destruction
A/S Ratio
A/S ratio does not control the basic ternary classification of the shoreline but is a key component in the stratigraphic record
Base level fall may increase sediment flux
Key
FIRST ORDER FACTOR
Second order factor
Second order factor that can be predicted in the ancient
Modern parameter used in this study
A
B
A controls B
A
C
A influences C

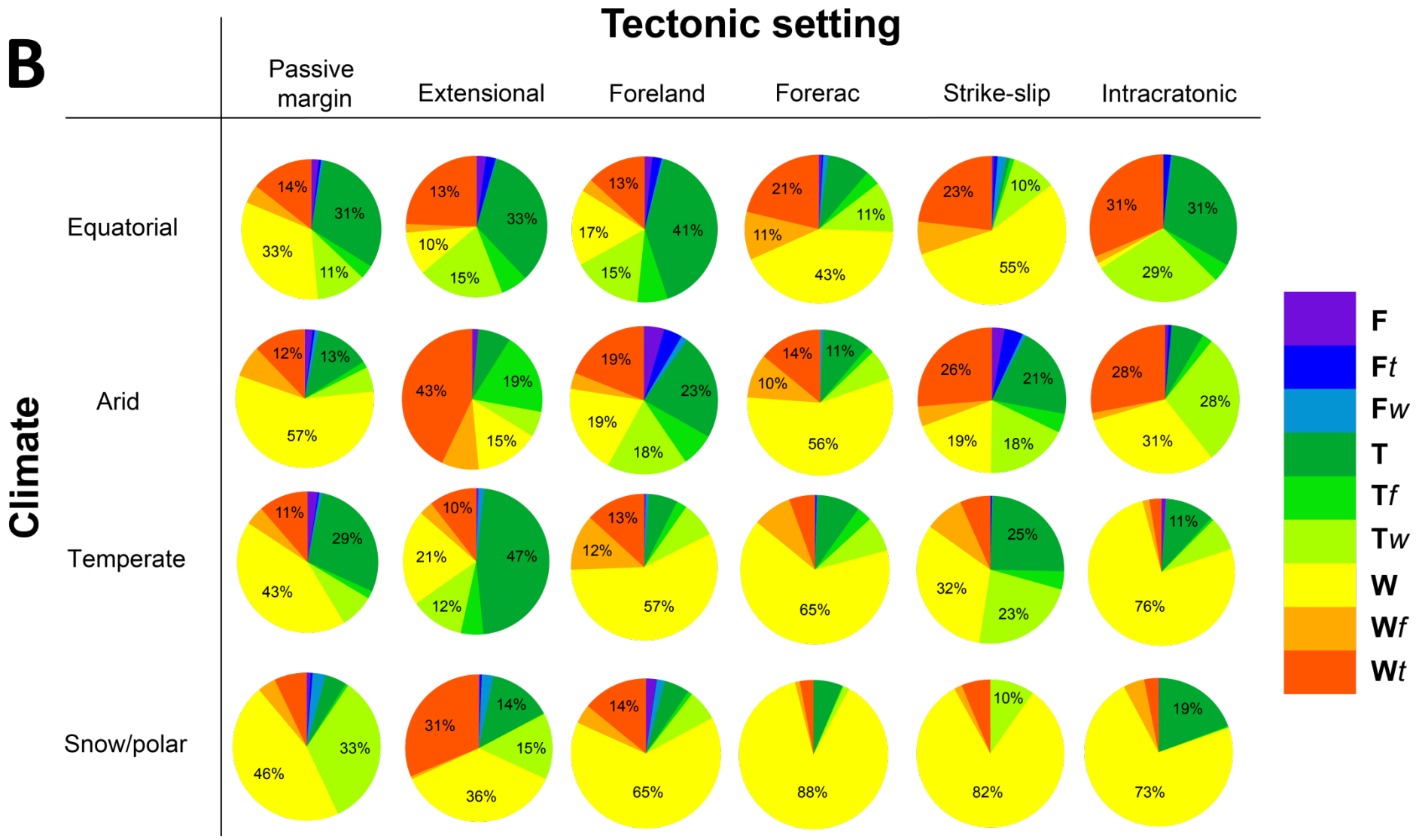
B
Tectonic setting
Passive margin
Extensional
Foreland
Forerac
Strike-slip
Intracratonic
Climate
Equatorial
Arid
Temperate
Snow/polar
14%
31%
33%
11%
13%
33%
10%
15%
13%
41%
17%
15%
21%
11%
11%
43%
23%
10%
55%
31%
31%
29%
12%
13%
57%
43%
19%
15%
19%
23%
19%
18%
14%
11%
10%
56%
26%
21%
19%
18%
28%
28%
31%
11%
29%
43%
10%
47%
21%
12%
13%
12%
57%
65%
25%
32%
23%
11%
76%
46%
33%
31%
14%
15%
36%
14%
65%
88%
10%
82%
19%
73%
F
Ft
Fw
T
Tf
Tw
W
Wf
Wt

Figure 23. (previous page) **A** shows the interplay between factors that influence shoreline typology. This is separated into first and second order controls including those parameters that can be predicted in the modern and ancient, namely climate and tectonics. **B** displays the relationship of climate and tectonics by ternary process from the modern. Percentages displayed where proportion is greater than 10%. This could be used to predict the probability of a particular shoreline type in a given climatic and tectonic setting.

Passive continental margins will tend to have broad shelves with relatively slow subsidence, increasing in a basinward direction. Passive margins commonly lay on the edge of large, stable continental landmasses with well established, drainage basins that deliver major volumes of sediment to the shoreline. The wide shelves will typical promote tidal conditions (Ainsworth et al., 2011). Active margins in fore arc settings will conversely be associated with narrow shelves and while newly uplifted mountains along the coastline will be an excellent source of sediment, an absence of large drainage systems will result in multiple, small delivery points (Milliman and Syvitski, 1992). Shorelines in rift, strike-slip and foreland basins will generally have lower basinal energy, although tidal amplification may occur in funnel shaped basins. Rates of accommodation creation are typically high and sediment supply is partitioned by complex topography at the shoreline. Consequently such systems are commonly aggradational to transgressive (e.g., Howell et al. 1996).

In summary, plate tectonics is the fundamental control on shoreline morphology, controlling latitude distribution of continental landmass, shelf width, ocean basin morphology and the A/S ratio (accommodation to supply) at the coastline. Secondary controls, which can be used predictively in the ancient, include climate and tectonic setting, which is a product of latitude, basin morphology and plate tectonics (Figure 23). A predicted shoreline ternary process, based on climate and tectonic controls (e.g., Figure 23B), should be applied with caution to the

subtleties in shoreline typology controls (Figure 23A) that may alter any given marginal marine geomorphology. The results described above suggest that a majority of modern depositional shorelines are wave dominated. Tidal systems are more likely in low to mid latitudes in basins with wide shelves or more complex morphologies. Fluvial dominated shorelines are rare and the major systems occur on passive margins and foreland basins (Figure 9, Figure 22; Figure 23).

The secondary goal of this study is to provide a systematic methodology for locating modern analogues for ancient reservoir systems. Outcrop analogues have long been used to provide important information on sediment body geometry and the lateral relationships between facies in cross section (see Howell et al. 2014 for a review). More recently the advent of freely available remote sensing data (e.g., Google Earth; Tooth, 2013) has seen a major increase in the use of modern analogues (e.g., Weissmann et al. 2010; Ainsworth et. 2011) to provide key information on the plan view geometries and relationships within systems. A key challenge remains the identification of suitable modern analogues. The maps presented in this paper (Fig 8) allow suitable process classified shoreline segments to be identified. This can be combined with additional information on climate (Table 3; Figure 23); tectonic setting (Table 4; Figure 21; Figure 23); latitude (Figure 13) or shelf width (Figure 18) to identify modern systems that can then be studied in greater detail to extract reservoir body dimensions.

Any study which uses modern systems as analogues must recognize that such studies detail the two-dimensional geometric, spatial and temporal evolution of sandbody elements and their relation to three-dimensional preservation. For instance, many deltas build behind barrier island complexes (Bhattacharya and Giosan, 2003) that volumetrically may become significant after continued wave-modification of an abandoned delta lobe prior to subsequent preservation. The identification of ternary processes on modern shorelines should therefore be applied in a context

of its broader depositional environment and preservation in space and time to find one or multiple suitable modern marginal marine analogues that relate to the sequences of preserved sedimentary deposition in the rock record.

8. Conclusions

This study has demonstrated a unique mapping of 927,577 km of shorelines from across the globe. Of this 28% are depositional, while the remaining 72% are rocky coastlines in net erosion. The shorelines have been further classified using a two tier, ternary classification based upon (Galloway, 1975; Ainsworth et al., 2011) which considers the relative importance of fluvial discharge, mean significant wave height and mean tidal range. The study has shown that the majority of coastlines are wave dominated with an increase in tidal systems towards the equator. Fluvial dominated systems make up a very small proportion of coastlines. More specifically:

1) Shorelines in net deposition are more mixed-influenced than their erosional shoreline counterparts and this observed difference has been accounted for by the algorithm. Depositional settings are more pronounced in the equatorial and mid-latitudes and thereby mix-influenced shorelines are more pronounced in those regions.

2) The highest frequency of fluvial outputs are likewise distributed along the equatorial and mid-latitudes. The major rivers of the world that are depositing into open bodies of water are typically tide-modified (**Ft**, **Tf**). In contrast, wave-modified fluvial shorelines (**Fw, Wf**) are of higher frequency though smaller discharge.

3) Wider shelves amplify tidal processes by threefold in comparison to narrow shelves, they also dampen wave energy.

4) Passive margins and foreland basins are globally the most representative distributions of tectonic regimes of shorelines. A significant portion of shorelines related to those tectonic regimes are of wide continental shelves with increased tidal modification. Fore-arc basins have narrow shelves that are dominated by Wave processes.

5) The energy environment of the marginal marine at present is related to the distribution of continents. This has created a restricted low basinal energy arctic that is mainly Wave-dominated erosional shorelines. Tidally-modified arctic shorelines typically develop in regions of unconsolidated sediment in funneled or restricted shoreline typologies. Higher energy, mixed-influenced ternary processes develop in equatorial and southern latitudes relating to open oceanic waterbodies.

6) Controls on shallow marine systems include a complex interplay between tectonic plates, climate, latitude, tectonic setting, shoreline morphology and A/S ratio.

The digitized global distribution of ternary process has shown the value in quantified information to derive new relationships on the fundamental controls that govern shoreline geomorphology. It has furthermore provided the means by which to find suitable modern analogues by ternary process, shelf width, latitude, tectonics and climate. These findings build on a continued realization towards a globally populated database of modern marginal marine geometric sandbody elements to improve models of sedimentary systems.

Acknowledgements

Support for this work came from the SAFARI consortium which was funded by Bayern Gas, ConocoPhillips, Dana Petroleum, Dong Energy, Eni Norge, GDF Suez, Idemitsu, Lundin, Noreco, OMV, Repsol, Rocksource, RWE, Statoil, Suncor, Total, PDO, VNG and the

Norwegian Petroleum Directorate (NPD). This manuscript has benefited from discussion with Bruce Ainsworth, Rachel Nanson and Christian Haug Eide. Boyan Vakarelov and Richard Davis Jr. are thanked for their constructive reviews and valuable comments that helped to improve the manuscript.

References

Ainsworth, R., Flint, S.S., Howell, J.A., 2008. Predicting Coastal Depositional Style: Influence of Basin Morphology and Accommodation To Sediment Supply Ratio Within A Sequence Stratigraphic Framework SPEM Spec. Publ. Recent Advances in Models of Siliciclastic Shallow-Marine Stratigraphy 90.

Ainsworth, R., Vakarelov, B., Nanson, R., 2011. Dynamic Spatial and temporal prediction of changes in depositional processes on clastic shorelines: Towards improved subsurface uncertainty reduction and management. AAPG Bulletin 95, 267-297.

Aviso, 2012. FES2012 was produced by Legos and CLS Space Oceanography Division and distributed by Aviso, with support from Cnes

Bhattacharya, J.P., Giosan, L., 2003. Wave-influenced deltas: geomorphological implications for facies reconstruction. Sedimentology 50, 187-210.

Bird, C.E., Franklin, E.C., Smith, C.M., Toonen, R.J., 2013. Between tide and wave marks: a unifying model of physical zonation on littoral shores. PeerJ 1, e154.

Bird, P., 2003. An updated digital model of plate boundaries. Geochemistry, Geophysics, Geosystems 4, 1027.

Boyd, R., Dalrymple, R., Zaitlin, B.A., 1992. Classification of clastic coastal depositional environments. Sedimentary Geology 80, 139-150.

Boyd, R., R.W. Dalrymple, and B.A. Zaitlin, B.A., 2006, Estuary and incised valley facies models, in Posamentier, H.W., and Walker, R.G., eds., Facies Models Revisited: SEPM, Special Publication 84,

p. 171–234.

Buddemeier, R.W., Smith, S.V., Swaney, D.P., Crossland, C.J., Maxwell, B.A., 2008. Coastal typology: An integrative “neutral” technique for coastal zone characterization and analysis. Estuarine, Coastal and Shelf Science 77, 197-205.

Carrère, L., Lyard, F., Cancet, M., Guillot, A., Roblou, L., 2012. FES2012: A new global tidal model taking taking advantage of nearly 20 years of altimetry, Proceedings of meeting "20 Years of Altimetry", Venice.

Clarke, A.J., Battisti, D.S., 1981. The effect of continental shelves on tides. Deep Sea Research Part A. Oceanographic Research Papers 28, 665-682.

Costanza, R., d'Arge, R., Groot, R.d., Farber, S., Grasso, M., Hannon, B., Limburg, K., Naeem, S., O'Neill, R.V., Paruelo, J., Raskin, R.G., Sutton, P., Belt, M.v.d., 1998. The value of the world's ecosystem services and natural capital. Nature 387, 253-260.

Cram, J.M., 1979. The Influence of Continental Shelf Width on Tidal Range: Paleoceanographic Implications. The Journal of Geology 87, 441-447.

Crossland, C.J., Kremer, H.H., Lindeboom, H.J., Crossland, J.I.M., LeTissier, M.D.A., 2003. Coastal fluxes in the Anthropocene. Global change the IGBP Series. Springer, Berlin.

Dalrymple, R.W., Zaitlin, B.A., Boyd, R., 1992. Estuarine facies models: conceptual basis and stratigraphic implications. Journal of Sedimentary Petrology 62, 1130–1146.

Danielson, J.J., Gesch, D.B., 2011. Global multi-resolution terrain elevation data 2010 (GMTED2010): U.S. Geological Survey Open-File Report 2011–107. 26.

Davies, J.L., 1964. A morphogenic approach to world shorelines. Z. Geomorphol. 8, 27-42.

Davis Jr, R.A., Hayes, M.O., 1984. What is a Wave-dominated coast? Marine Geology 60, 313-329.

Davis Jr, R.A., 2013. A New Look at Barrier-Inlet Morphodynamics. Journal of Coastal Research: Special Issue 69 - Proceedings, Symposium in Applied Coastal Geomorphology to Honor Miles O. Hayes, 1 – 12.

Deveugle, P.E.K., Jackson, M.D., Hampson, G.J., Stewart, J., Clough, M.D., Ehighebolo, T., Farrell,

M.E., Calvert, C.S., Miller, J.K., 2014. A comparative study of reservoir modeling techniques and their impact on predicted performance of Fluvial-dominated deltaic reservoirs. AAPG Bulletin 98, 729-763.

Dickinson, W.R., 1974. Plate tectonics and sedimentation. Society of Economic Paleontologists and Mineralogists Special Publication 22, 1-27.

Dürr, H., Laruelle, G., van Kempen, C., Slomp, C., Meybeck, M., Middelkoop, H., 2011. Worldwide Typology of Nearshore Coastal Systems: Defining the Estuarine Filter of River Inputs to the Oceans. Estuaries and Coasts 34, 441-458.

Dürr, H.H., Meybeck, M., Dürr, S.H., 2005. Lithologic composition of the Earth's continental surfaces derived from a new digital map emphasizing riverine material transfer. Global Biogeochemical Cycles 19, GB4S10.

Eide, C.H., Howell, J., Buckley, S., 2014. Distribution of discontinuous mudstone beds within wave-dominated shallow-marine deposits: Star Point Sandstone and Blackhawk Formation, Eastern Utah The American Association of Petroleum Geologists Bulletin 98, 1401-1429.

Enge, H.D., Howell, J.A., 2010. Impact of deltaic clinothems on reservoir performance: dynamic studies of reservoir analogs from the Ferron Sandstone Member and Panther Tongue, Utah. AAPG Bulletin 94, 139-161.

ESRI, 2014. ESRI (Environmental Systems Resource Institute). 2014. ArcMap 10.1. ESRI, Redlands, California.

Fekete, B.M., Vörösmarty, C.J., Grabs, W., 2002. High-resolution fields of global runoff combining observed river discharge and simulated water balances. Global Biogeochemical Cycles 16, 15-11-15-10.

Galloway, W.E., 1975. Process Framework for Describing the Morphologic and Stratigraphic Evolution of Deltaic Depositional Systems, Deltas: Models for Exploration, 1975. Houston Geological Society, Houston, Texas, pp. 87-98.

Global Runoff Data Centre, 2007. Major River Basins of the World / Global Runoff Data Centre.

Koblenz, Federal Institute of Hydrology (BfG).

Goodbred, S., Jr., Saito, Y., 2012. Tide-Dominated Deltas, in: Davis Jr, R.A., Dalrymple, R.W. (Eds.), Principles of Tidal Sedimentology. Springer Netherlands, pp. 129-149.

Hampson, G.J., Storms, J.E.A., 2003. Geomorphological and sequence stratigraphic variability in wave-dominated, shoreface-shelf parasequences. Sedimentology 50, 667-701.

Harris, P.T., Heap, A.D., Bryce, S.M., Porter-Smith, R., Ryan, D.A., Heggie, D.T., 2002. Classification of Australian Clastic Coastal Depositional Environments Based Upon a Quantitative Analysis of Wave, Tidal, and River Power Journal of Sedimentary Research 6, 858-870.

Hartmann, J., Moosdorf, N., 2012. The new global lithological map database GLiM: A representation of rock properties at the Earth surface. Geochemistry, Geophysics, Geosystems 13, Q12004.

Hay, W.W., 1996. Tectonics and climate. Geol Rundsch 85, 409-437.

Hori, K., Saito, Y., Wang, P., 2002. Architecture and evolution of the tide-dominated Changjiang (Yangtze) River delta, China. Sedimentary Geology 146, 249-264.

Howell, J., Skorstad, A., MacDonald, A., Fordham, A., Flint, S., Fjellvoll, B., Manzocchi, T., 2008. Sedimentological parameterization of shallow-marine reservoirs. Petroleum Geoscience 14.

Howell, J.A., Flint, S.S., Hunt, C., 1996. Sedimentological aspects of the Humber Group (Upper Jurassic) of the South Central Graben, UK North Sea. Sedimentology 43, 89-114.

Howell, J.A., Martinius, A.W., Good, T.R., 2014. The application of outcrop analogues in geological modelling: a review, present status and future outlook. Sediment-Body Geometry and Heterogeneity: Analogue Studies for Modelling the Subsurface. Geological Society, London, Special Publications 387.

Ingersoll, R.V., 2012. Tectonics of sedimentary basins with revised nomenclature, in: Bursby, C., Azor, A. (Eds.), Tectonics of Sedimentary Basins Recent Advances, First Edition ed. Blackwell Publishing Ltd, Chichester, West Sussex, pp. 3-43.

Inman, D.L., Nordstrom, C.E., 1971. On the Tectonic and Morphologic Classification of Coasts. The Journal of Geology 79, 1-21.

Jorgenson, M.T., Brown, J., 2005. Classification of the Alaskan Beaufort Sea Coast and estimation of carbon and sediment inputs from coastal erosion. Geo-Mar Lett 25, 69-80.

Kottek, M., 2006. World map of the Köppen-Giger climate classification updated. Meterologische Zeitschrift 15, 259-263.

Lehner, B., Verdin, K., Jarvis, A., 2008. New Global Hydrography Derived From Spaceborne Elevation Data. Eos, Transactions American Geophysical Union 89, 93-94.

Longhitano, S.G., Mellere, D., Steel, R.J., Ainsworth, R.B., 2012. Tidal depositional systems in the rock record: A review and new insights. Sedimentary Geology 279, 2-22.

Martinius, A. W., Ravnås, R., Howell, J. A., Steel, R. J., and Wonham, J. P., 2014, From Depositional Systems to Sedimentary Successions on the Norwegian Continental Margin, John Wiley & Sons, Special Publication Number 46 of the International Association of Sedimentologists.

McIlroy, D., Flint, S., Howell, J.A., Timms, N., 2005. Sedimentology of the tide-dominated Jurassic Lajas Formation, Neuquén Basin, Argentina. Geological Society, London, Special Publications 252, 83-107.

Menot, L., Sibuet, M., Carney, R.S., Levin, L.A., Rowe, G.T., Billett, D.S.M., Poore, G., Kitazato, H., Vanreusel, A., Galéron, J., Lavrado, H.P., Sellanes, J., Ingole, B., Krylova, E., 2010. New Perceptions of Continental Margin Biodiversity, Life in the World's Oceans. Wiley-Blackwell, pp. 79-102.

Milliman, J.D., Syvitski, J.P.M., 1992. Geomorphic/Tectonic Control of Sediment Discharge to the Ocean: The Importance of Small Mountainous Rivers. The Journal of Geology 100, 525-544.

Mørk, G., Barstow, S., Kabuth, A., Pontes, T., 2010. Assessing the global wave energy potential, Proc. of OMAE2010, 29th International Conference on Ocean, Offshore Mechanics and Arctic Engineering, Shanghai, China.

Nanson, R., Ainsworth, R., Vakarelov, B., Fernie, J., Massey, A., 2012. Geometric attributes of reservoir elements in a modern, low accommodation, tide-dominated delta. APPEA Journal, 483-492.

Nanson, R.A., Vakarelov, B.K., Ainsworth, R.B., Williams, F.M., Price, D.M., 2013. Evolution of a

Holocene, mixed-process, forced regressive shoreline: The Mitchell River delta, Queensland, Australia. Marine Geology 339, 22-43.

NASA LP DAAC, 2001. NASA Land Processes Distributed Active Archive Center (LP DAAC) USGS/Earth Resources Observation and Science (EROS) Center. MOD 11 - Land Surface Temperature and Emissivity

Nyberg, B., Howell, J.A., 2015. Is the present the key to the past? A global characterization of modern sedimentary basins, Geology 43, 643-646.

Orton, G.J., Reading, H.G., 1993. Variability of deltaic processes in terms of sediment supply, with particular emphasis on grain size. Sedimentology 40, 475-512.

Overeem, I., Anderson, R.S., Wobus, C.W., Clow, G.D., Urban, F.E., Matell, N., 2011. Sea ice loss enhances wave action at the Arctic coast. Geophysical Research Letters 38, L17503.

Reuter, H.I., Nelson, A., Jarvis, A., 2007. An evaluation of void ‐ filling interpolation methods for SRTM data. International Journal of Geographical Information Science 21, 983-1008.

Short, A.D., 2006. Australian Beach Systems—Nature and Distribution. Journal of Coastal Research 22, 11-27.

Sperner, B., Müller, B., Heidbach, O., Delvaux, D., Reinecker, J., Fuchs, K., 2003. Tectonic stress in the Earth's crust: advances in the World Stress Map project. - In: Nieuwland D. (ed.): New insights into structural interpretation and modelling. Geological Society of London Special Publications 212, 101-116.

Syvitski, J.P.M., Milliman, J.D., 2007. Geology, Geography, and Humans Battle for Dominance over the Delivery of Fluvial Sediment to the Coastal Ocean. The Journal of Geology 115, 1-19.

Talaue-McManus, L., Smith, S.V., Buddemeier, R.W., 2003. Biophysical and socio-economic assessments of the coastal zone: the LOICZ approach. Ocean & Coastal Management 46, 323-333.

Tolman, H.L., 2002. Validation of WAVEWATCH III Version 1.15 for a Global Domain. NOAA/NWS/NCEP/OMB Technical Note Nr. 213, p. 33.

Tooth, S., 2013. 14.5 Google Earth™ in Geomorphology: Re-Enchanting, Revolutionizing, or Just another Resource?, in: Shroder, J.F. (Ed.), Treatise on Geomorphology. Academic Press, San Diego, pp. 53-64.

Tye, R.S., 2004. Geomorphology: An approach to determining subsurface reservoir dimensions. AAPG Bulletin 88, 1123 -1147.

Vafeidis, A.T., Nicholls, R.J., McFadden, L., Tol, R.S.J., Hinkel, J., Spencer, T., Grashoff, P.S., Boot, G., Klein, R.J.T., 2008. A New Global Coastal Database for Impact and Vulnerability Analysis to Sea-Level Rise. Journal of Coastal Research, 917-924.

Vakarelov, B.K. and Ainsworth, R.B., 2011. Predicting Marginal Marine Reservoir Architecture: Examples from Asian Shoreline Systems. IPTC Meeting, Bangkok, Thailand, February 2012.

Vakarelov, B.K., Ainsworth, R.B., 2013. A hierarchical approach to architectural classification in marginal-marine systems: Bridging the gap between sedimentology and sequence stratigraphy. AAPG Bulletin 97, 1121-1161.

Vakarelov, B.K., Ainsworth, R.B., MacEachern, J.A., 2012. Recognition of Wave-dominated, tide-influenced shoreline systems in the rock record: Variations from a microtidal shoreline model. Sedimentary Geology 279, 23-41.Van Wagoner, J.C., Mitchum, R.M., Campion, K.M., Rahmanian, V.D., 1990. Siliciclastic Sequence Stratigraphy in Well Logs, Cores, and Outcrops: Concepts for High-Resolution Correlation of Time and Facies: AAPG Methods in Exploration 7., Tulsa, USA.

Vörösmarty, C.J., Fekete, B.M., Meybeck, M., Lammers, R.B., 2000a. Geomorphometric attributes of the global system of rivers at 30-minute spatial resolution. Journal of Hydrology 237, 17-39.

Vörösmarty, C.J., Fekete, B.M., Meybeck, M., Lammers, R.B., 2000b. Global system of rivers: Its role in organizing continental land mass and defining land-to-ocean linkages. Global Biogeochemical Cycles 14, 599-621.

Weissmann, G.S., Hartley, A.J., Nichols, G.J., Scuderi, L.A., Olson, M., Buehler, H., Banteah, R., 2010. Fluvial form in modern continental sedimentary basins: Distributive fluvial systems. Geology 38, 39-42.

Wellner, R., Beaubouef, R., Wagoner, J.V., Roberts, H., Sun, T., 2005. Jet-Plume Depositional Bodies—The Primary Building Blocks of Wax Lake Delta. Gulf Coast Association of Geological Societies Transactions 55, 867-909.

Wessel, P., Smith, W., 1996. A global, self-consistent, hierarchical, high-resolution shoreline database. Journal of Geophysical Research 101, 8741-8743.

Wright, L.D., Coleman, J.M., 1973. Variations in morphology of major river deltas as functions of ocean wave and river discharge regimes. AAPG Bulletin 57, 370 - 398.

Zoback, M.L., 1992. First- and second-order patterns of stress in the lithosphere: The World Stress Map Project. Journal of Geophysical Research: Solid Earth 97, 11703-11728.